THE ZERO FREQUENCY RESPONSE OF SEA LEVEL TO METEOROLOGICAL INFLUENCES

C. L. MERRY
P. VANICEK

October 1981

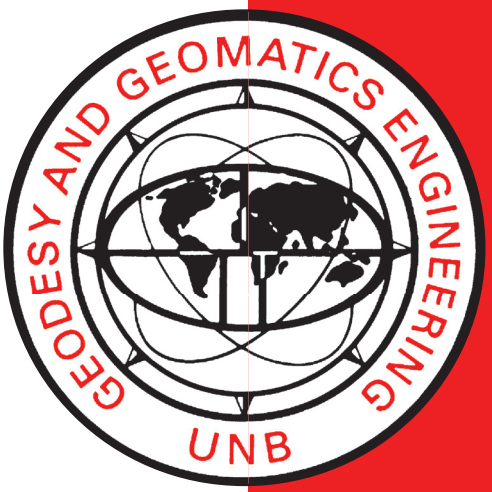

TECHNICAL REPORT
NO. 82

PREFACE

In order to make our extensive series of technical reports more readily available, we have scanned the old master copies and produced electronic versions in Portable Document Format. The quality of the images varies depending on the quality of the originals. The images have not been converted to searchable text.

THE ZERO FREQUENCY RESPONSE OF SEA LEVEL TO METEOROLOGICAL INFLUENCES

C.L. Merry and P. Vanicek

University of New Brunswick

Department of Surveying Engineering

Technical Report #82

October, 1981

ACKNOWLEDGEMENTS

The major computer program used for this study consists of a slightly modified version of the program SPANEQ, developed by Mr. R.R. Steeves. Permission to make use of his program is gratefully acknowledged.

Data used in this research was provided by a number of agencies, including the Canadian government departments of the Environment and Energy, Mines and Resources. We would especially like to thank the following for their assistance in locating and providing data:

Dr. P. Balbraith (Environment Canada) - pressure and temperature data

Mr. M. Webb (Environment Canada) - wind data

Mr. J. Naar (Fisheries and Oceans) - tide gauge data

Assistance with various aspects of data collection, programming and drafting was provided by Mr. A. Mbegha, Ms. I. Paim and Ms. V. Rinco.

This research was partially funded through strategic research grant on Marine Geodesy, provided by the Canadian National Science and Engineering Research Council. The first author (CLM) would like to acknowledge the support provided by a South African Council for Scientific and Industrial Research Postdoctoral Scholarship, while on research and study leave from the University of Cape Town.

TABLE OF CONTENTS

LIST OF FIGURES

List of Tables

CHAPTER ONE

INTRODUCTION

1.1 Levelling Datum

The primary reference surface for heights is the geoid. The geoid is defined as that equipotential surface of the earth's actual gravity field which most closely approximates the mean sea level in the spatial least squares sense, where the mean sea level (MSL) is the mean (surface) of all the instantaneous sea surfaces during a period $T \equiv (\tau - \Delta\tau/2, \tau + \Delta\tau/2)$. Thus the MSL is a function of time, i.e. $MSL^{(T)}$. It can be located, i.e., its height with respect to arbitrary reference surface determined, at any point as a temporal mean of all the instantaneous sea level heights during the period T. These instantaneous sea level heights are recorded by tide gauges, with respect to a nearby reference bench mark. Therefore, it is only at the tide gauges that the height of MSL (T) can be located.

The departure of the MSL (T) from the geoid is called sea surface topography (SST). The causes of the SST(T) include ocean currents, water density variations due to salinity and temperature, and meteorological variations such as the air pressure and wind stress. In addition, close to the shore, the sea-bed topography and river discharge may also play significant roles.

The practical realization of the geoid is brought about by tide gauge measurements at selected points. The effects of tides, and of other periodic influence can be filtered out using appropriate filters. Typically, 18.6 years has been used as the averaging time (corresponding to the period of precession of the

lunar nodes), but equivalent results may be obtained using shorter periods [Vanicek, 1978]. Clearly, mean sea level as obtained in this fashion will still be burdened with the SST, at the tide gauge site, and will not correspond with the geoid. It may be argued that this is immaterial, because it is close to the geoid, and is thus sufficient for most practical purposes. However, it has been the practice to connect precise levelling nets to several tide gauges, widely dispersed around the perimeter of the net. The sea-surface topography at each tide gauge is different, and the resulting adjustment of the levelling data to fit these different m.s. levels can lead, and has led, to distortions in the level networks.

1.2 Modelling of Sea-Surface Topography

One obvious solution to this problem of relating the reference surface at tide gauge sties to the MSL is to model the sea surface topography at each site. Great strides have been made on the application of satellite-based radar altimeters for this purpose (e.g. Delikaraoglou, 1980). However, the accuracy achievable with this technique is still an order of magnitude too low for our purpose (we would like to achieve better than 10 cm accuracy), and, in any case, it is doubtful whether the results of open ocean satellite altimetry could be extrapolated reliably to the land/sea interface.

Another approach, consisting of measuring variations in temperature and salinity with depth along a profile exists. It is called "steric levelling" and can be used only in deep sea, where the necessary assumption of no horizontal currents at the reference isobaric surface at depth may be justifiable. Even then there are some serious doubts about the validity of the technique.

An alternative technique, proposed here, is to make use of the response of sea level to external effects, such as atmospheric pressure, temperature, wind, etc. This response can be modelled in two components (amplitude factor, and phase lag), as a function of frequency. The response method, described in the next chapter, has been used in the field of electrical engineering for some time, but has only recently been introduced into oceanography [Munk and Cartwright, 1966]. Munk and Cartwright, and subsequent investigators, have used this technique principally to model the response of sea level to the high frequency phemonena (diurnal and semi-diurnal tides). In the approach envisaged here, the response would be modelled in the low-frequency. The zero frequency response can be used to estimate the quasi-stationary sea surface topography, knowing the quasi-stationary departures (long-term means) of the forcing parameters.

In order to evaluate the technique, mean sea level and other data for several tide gauges in the Maritime provinces of Canada have been collected. These data include atmospheric pressure, air temperature, river discharge, and wind observations at various sites. Neither water temperature nor salinity records were available at the tide gauge sites, and it was beyond the competence of the investigators to evaluate the influence of ocean currents (see, e.g. Lisitzin, 1974) and the shape of the sea-level. This question, it was felt, falls entirely into the domain of physical oceanographers. Consequently, the results obtained here are incomplete in so far that they do not represent the entire sea surface topography at the tide gauges. They should, however, reflect its local variations.

CHAPTER TWO

RESPONSE METHODS

This chapter is concerned with the description of three different methods for determining the frequency-dpendent response of a physical system to an imput (forcing) function. The situation considered is that in which the input function is known, as a time series, x(t), and the output function is known (or measured) as a time series, y(t). As an example, a time series representing the gravitational potential of the sun and moon may be the input to a physical system represented by the sea, and the output series may be the measured tides at a point.

The methods to be described are those of cross-spectral analysis [Bendat and Piersol, 1971], in which the statistical coherence of the input and output series is used; the weighting function approach [Munk and Cartwright, 1966], which is essentially the same as the first technique, except that computations are carried out in the time domain, instead of the frequency domain; and the least squares response analysis [Steeves, 1981a], in which the response is determined at pre-defined frequencies only.

In addition to the description of these methods, a numerical comparison, in which particular attention is paid to the influence of noise is also described, and the reasons for the final selection of method are outlined.

2.1 Cross-Spectral Analysis

The method of cross-spectral analysis is well-known in the field of electrical engineering, and will only be described briefly here. Most of the content of this section has been inspired by the text by Bendat and Piersol [1971].

The response of a physical system can be modelled in both the time and frequency domains. In the time domain we can write

$$y(t) = \int_{-\infty}^{+\infty} h(\tau)\, x(t-\tau)\, d\tau \tag{2.01}$$

where, h(t), the quantity we are after, is called the weighting function, or impulse response function, and describes the physical characteristics of the system.

In the frequency domain, the frequency response function (or admittance function), H(f) is the Fourier Transform of $h(\tau)$:

$$H(f) = \int_{\infty}^{\infty} h(\tau) e^{-i2\pi f\tau}\, d\tau \,. \tag{2.02}$$

It can be shown [Papoulis, 1962] that:

$$H(f) = \frac{G_{xy}(f)}{G_{xx}(f)} \,, \tag{2.03}$$

where $G_{xx}(f)$ and $G_{xy}(f)$ are the power spectral and cross-spectral density functions of x(t) and y(t). These quantities are related to the Fourier transforms of the corresponding auto- and cross-covariance functions by the expressions:

$$\begin{aligned} G_{xx}(f) &= 2\int_{-\infty}^{\infty} R_{xx}(\tau)\, e^{-i2\pi f\tau} d\tau \\ G_{xy}(f) &= 2\int_{-\infty}^{\infty} R_{xy}(\tau)\, e^{-i2\pi f\tau} d\tau \,. \end{aligned} \tag{2.04}$$

The functions, $R_{xx}(\tau)$ and $R_{xy}(\tau)$ are given by:

$$R_{xx}(\tau) = \lim_{T\to\infty} \frac{1}{T} \int_o^T x(t).x(t+\tau)\, d\tau$$

$$R_{xy}(\tau) = \lim_{T\to\infty} \frac{1}{T} \int_o^T x(t).y(t+\tau)\, d\tau \quad . \tag{2.05}$$

Both $G_{xy}(f)$ and $H(f)$ are complex-valued functions, and H may be represented in the form:

$$H(f) = |H(f)|e^{-i\Phi(f)} \quad . \tag{2.06}$$

Here, $|H(f)|$ is the amplitude response (or gain factor) and $\Phi(f)$ is the phase response (or phase lead). $|H(f)|$ represents the ratio of amplitudes of the input and output series, at the frequency f (taken in the sense: output/input). Similarly, $\Phi(f)$ represents the phase difference (output-input) at the frequency, f.

The approximate evaluation of H(f) could be carried out directly using equations (2.03) to (2.05) replacing the integrations by summations, with appropriate limits. In practice, $G_{xy}(f)$ and $G_{xx}(f)$ can be determined directly from the time series x(t) and y(t) using the Fast Fourier Transform technique. It is not considered appropriate to describe this technique here. However, details may be found in Bendat and Piersol [1971].

The above brief description covers the case of a single input, single output system. In practice, the more common situation is that of a multiple input, single output system (multichannel problem). Again, as an example, consider sea level as measured by a tide gauge. This produces a single output, y(t), but is influenced

by multiple inputs (such as the gravitational potential of the sun and moon, atmospheric pressure, winds, etc.). In this case, the formapism must be extended to cover the multiple correlations occurring between the different input series, $x_1(t)$, $x_2(t)$,...$x_n(t)$. This is achieved by considering all cross-spectral relationships in a spectral matrix equation:

$$\underline{H}(f) = \underline{G}_{xx}^{-1}(f) \cdot \underline{G}_{xy}(f) \tag{2.07}$$

where: $\underline{H}(f)$ is the vector of response functions:

$$\underline{H}(f) = \begin{bmatrix} H_1(f) \\ H_2(f) \\ \cdot \\ \cdot \\ H_n(f) \end{bmatrix} , \tag{2.08}$$

$\underline{G}_{xx}(f)$ is the matrix of cross-spectra between input functions:

$$\underline{G}_{xx}(f) = \begin{bmatrix} G_{11}(f) & G_{12}(f) & \cdots & G_{1n}(f) \\ G_{21}(f) & G_{22}(f) & \cdots & G_{2n}(f) \\ & \cdots\cdots\cdots\cdots & & \\ G_{n1}(f) & \cdots\cdots\cdots\cdots & & G_{nn}(f) \end{bmatrix} , \tag{2.09}$$

and $\underline{G}_{xy}(f)$ is the vector of cross-spectra between the input functions and the output function:

$$\underline{G}_{xy}(f) = \begin{bmatrix} G_{1y}(f) \\ G_{2y}(f) \\ \vdots \\ G_{ny}(f) \end{bmatrix} . \tag{2.10}$$

If the input functions are uncorrelated, $\underline{G}_{xx}(f)$ becomes diagonal, and the solution reduces to that of evaluating equation (2.03) n-times.

As for the single-input case, in practice the cross-spectra would be determined using the Fast Fourier Transform.

2.2 Weighting Function Approach

This method, developed by Munk and Cartwright (1966), is basically a modification of the previous method, and uses as its starting point the same convolution integral of equation (2.01), repeated here:

$$y(t) = \int_{-\infty}^{\infty} h(\tau)\ x(t-\tau)\ d\tau \ . \qquad (2.01)$$

In this approach, the form of the weighting function, h(t), is assumed known, and a solution is made for a finite number of coefficients of this function. After some experimentation, Munk and Cartwright adopted a simple weighting function consisting of a sequence of weights W_s, so that:

$$\hat{y}(t) = \sum_{s=-S}^{+S} W_s\ x\ (t-s\,\Delta\tau) \ . \qquad (2.11)$$

In this formulation, an arbitrary number of lags (2S+1 in total) and a fixed lag interval, $\Delta\tau$, are chosen. The unknown weights W_s, can be obtained using the least squares principle. This leads to a set of normal equations in W_s, which can be solved using conventional matrix algebra. Denoting by angle brackets scalar products of functions we get:

$$< x(t-s\Delta\tau),\ x(t-s\Delta\tau)> \cdot\ W_s = < x(t-s\Delta\tau),\ y(t)> \ . \qquad (2.12)$$

Once the weights are known, the discrete Fourier Transforms can be used to determine the response function, H(f):

$$H(f) = \sum_{s=-S}^{+S} W_s e^{-i2\pi fs\Delta\tau} \qquad (2.13)$$

or, separating into real and imaginary parts:

$$\begin{aligned} \mathrm{re}(H(f)) &= \sum_{s=-S}^{+S} W_s \cos(2\pi f s \Delta\tau) \\ \mathrm{im}(H(f)) &= \sum_{s=-S}^{+S} W_s \sin(2\pi f s \Delta\tau) \quad . \end{aligned} \tag{2.14}$$

The amplitude and phase responses are then:

$$\begin{aligned} |H(f)| &= (\mathrm{re}(H(f)^2) + \mathrm{im}(H(f)^2)^{\frac{1}{2}} \\ \Phi(f) &= \arctan\left(\frac{\mathrm{im}\ H(f)}{\mathrm{re}\ H(f)}\right) \quad , \end{aligned} \tag{2.15}$$

In actual usage, Munk and Cartwright (1966) and Cartwright (1969) have represented the input series by a complex-valued harmonic function, and have used the time-varying coefficients of this function in equation (2.12), rather than the time series itself. Concurrently, they have used complex-valued weights.

In the case of multiple-inputs, two approaches are possible. Cartwright (1969) has used cross-spectral analysis to determine the response functions (equations 2.07 and 2.08) and has then determined the weights by an inverse Fourier transform of the $H_j(f)$:

$$W_j(\tau) = 2 \int_o^\infty H_j(f)\, e^{i2\pi\tau f}\, df \quad . \tag{2.16}$$

As this approach uses the same equations as that of the cross-spectral analysis, there is no difference in the estimation of the response functions. Alternatively, Munk and Cartwright (1966), have extended the weighting function formulation to include multiple inputs:

$$y(t) = \sum_{j=1}^{n} \sum_{s=-S}^{+S} W_{js}\, x_j(t-s\Delta\tau) \tag{2.17}$$

and formed the normal equations:

$$\sum_{j=1}^{n} \langle x_k(t-s\Delta\tau),\, x_j(t-s\Delta\tau)\rangle \cdot W_{js} = \langle x_k(t-s\Delta\tau),\, y(t)\rangle \quad k=1,\ldots,n \qquad (2.18)$$

(for all s).

Then, for each input function:

$$H_j(f) = \sum_{s=-S}^{+S} W_{js}\, e^{-i2\pi fs\Delta\tau} \quad . \qquad (2.19)$$

2.3 Least Squares Response Analysis

This method (Steeves, 1981a) makes use of the spectral analysis technique developed by Vaníček (1971), and differs from the previous two methods in that the response function is only calculated at selected frequencies, f_i (i=1,..., m). The input and output series are modelled by trigonometric series of the form:

$$x(t) = \sum_{i=1}^{m} A_i \cos(2\pi f_i t - \gamma_i) + n_x(t) \quad , \qquad (2.20a)$$

$$y(t) = \sum_{i=1}^{m} B_i \cos(2\pi f_i t - \gamma_i) + n_y(t) \quad . \qquad (2.20b)$$

Here, the terms $n_x(t)$, $n_y(t)$ represent the residual random and systematic noise, which may or may not be modelled.

The selection of the particular frequencies, f_i, to be used comes from the spectral analysis of the input time series. It is not the intention to provide a detailed description of the least squares spectral analysis here. Details of the theory may be found in Vaníček (1971), and of the computer algorithms in Wells and Vaníček (1978). However, for the sake of completeness, a brief summary is presented here. For the least squares spectral analysis, the series x(t) is assumed to be represented by:

$$\hat{x}(t) = \sum_{i=1}^{\ell+2} c_i \Phi_i(t), \qquad (2.21)$$

where the $\Phi_i(t)$ are base functions of known form, with unknown coefficients, c_i. In particular, the last two terms are given by:

$$\Phi_{\ell+1}(t) = \cos 2\pi ft \ ,$$
$$\Phi_{\ell+2}(t) = \sin 2\pi ft \ , \qquad (2.22)$$

where f is that particular frequency at which the spectrum of x(t) is desired. The first ℓ base functions $\Phi_i(t)$ may represent datum biases, common or different for different parts of the series, ($\Phi_i(t) = 1$), linear trend ($\Phi_i(t) = t$) or more complex known constituents (even other known trigonometric terms). The coefficients c_i can be found by applying the least squares principle to equation (2.21), yielding the soluble set of normal equations:

$$\sum_{S=1}^{\ell+2} < \Phi_i(t), \Phi_j(t) > \cdot c_j = < \Phi_i(t), \hat{x}(t) > \quad i = 1, \ldots, \ell+2 \qquad (2.23)$$

Back-substituting the c_i into (2.21) enables $\hat{x}(t)$ to be evaluated for all t. Provided a suitable choice of the ϕ_i has been made, $\hat{x}(t)$ should be "close" to x(t). The closeness may be quantified using the least-squares norm of $x(t) - \hat{x}(t)$, i.e.:

$$\sum_{t_i} (x(t_i) - x(t_i))^2 . \qquad (2.24)$$

Equations (2.21 - 2.24) may be re-used with the summation extending to ℓ only (i.e. the functions $\Phi_{\ell H}$, $\Phi_{\ell+2}$ are dropped).

In this case, we have another representation of x(t) given by:

$$\hat{x}'(t) = \sum_{i=1}^{\ell} c_i' \Phi_i(t) \ . \qquad (2.25)$$

This leads to another norm:

$$\| x(t) - \hat{x}'(t) \| \ . \qquad (2.26)$$

If the terms $\Phi_{\ell+1}$, $\Phi_{\ell+2}$ contribute significantly to x(t) $||x-\hat{x}||$ will be significantly smaller than $||x-\hat{x}'||$, and their ratio provides us with a measure of the contribution of the particular frequency, f, to the spectrum of x(t). Specifically, the spectrum is given by:

$$S(f) = 1 - ||x(t) - \hat{x}'(t)||^2 \; / \; ||x(t) - \hat{x}(t)||^2 . \qquad (2.27)$$

In order to obtain a complete spectrum, equations (2.21 - 2.27) would have to be evulated for all values of f. In practice, a more optimal algorithm may be used, so that equation (2.23) need be solved only once (Wells and Vaníček, 1978).

Returning to the determination of the frequency response, the least-squares spectral analysis is used to determine the predominant frequencies in x(t), by means of equation (2.27), and can also be used to determine the amplitudes and coefficients, A_i, γ_i, of equation (2.20), by using the appropriate base functions in equation (2.21). The same algorithms may be used to determine the coefficients, B_i, ψ_i, in y(t), at the common frequencies f_i. Note that other frequencies may be present in y(t), and should be determined and modelled simultaneously.

Once the constituents of (2.20) have been determined, the amplitude and phase responses at the selected frequencies, f_i are given by:

$$\begin{aligned} |H(f_i)| &= \frac{A_i}{B_i} \quad , \\ \Phi(f_i) &= \gamma_i - \psi_i \quad . \end{aligned} \qquad (2.28)$$

In the case of multiple inputs, the least squares spectral analysis is easily extended. For the n input series $x_1(t)$, $x_2(t),\ldots,x_n(t)$, a spectral analysis is carried out to determine the predominant frequencies in each input. All these frequencies are then used simultaneously in (2.20b), to arrive at n sets of responses. It should be pointed out that, as with the other response methods, it is not possible to resolve the contributions at frequencies common to more than one input series.

2.4 Comparison of the Response Methods

A complete comparison of the three response methods discussed above has not been carried out. Present comparison is restricted to a numerical evaluation of the behaviour of the methods under the influence of noise, using generated test series. No attempt has been made at a theoretical analysis, nor at using more than one input series in the numerical testing.

Two test data sets were generated, representing input and output series:

$$x(t_j) = a_o + \sum_{i=1}^{3} A_i \cos(2\pi f_i t_j - \gamma_i) + n_x(t_j)$$

$$y(t_j) = b_o + \sum_{\ell=1}^{3} B_\ell \cos(2\pi f_\ell t_j - \gamma_\ell) + n_y(t_j) \qquad (2.29)$$

$$(j = 1,\ldots, 1024).$$

Two of the three frequencies were common to x(t) and y(t). The noise series, $n_x(t)$ and $n_y(t)$, were calculated using a random number generator, with zero mean, and varying scale factors. These scale factors were applied such that the noise/signal ratio was varied from 0.0 to 2.0. This ratio is given by:

$$r = \frac{\text{RMS noise}}{\text{RMS signal}} = \left(\frac{\sum_{i=1}^{1024} (n_x(t_i))^2}{\sum_{i=1}^{1024} (x(t_i) - n_x(t_i))^2} \right)^{1/2} . \qquad (2.30)$$

For the cross-spectral analysis, available computer subroutines (IMSL package at the University of New Brunswick Computer Centre) for $G_{xy}(f)$ and $G_{xx}(f)$ were used. These routines employ a Fast Fourier Transform algorithm, with ensemble averaging, resulting in some reduction of spectral resolution.

In the weighting function approach, equations (2.11 to 2.15) were programmed, with the modification that the range of s was restricted to non-negative values (i.e. causality was maintained). Different values for Δt and S were experimented with, and best results were obtained for $\Delta t = t_{i+1} - t_i$, and S in excess of 9 (a value of S = 12 was finally adopted). For both this method and the cross-spectral analysis, the datum biases a_o and b_o had to be removed first, by subtracting the means of each of x(t) and y(t).

For the least squares response analysis, an extension of Wells and Vaníček (1978) algorithm, developed by Steeves (1981a) was used. The datum biases could be treated as base functions with unknown coefficients determined in the general solution for the spectrum.

For each method, the amplitude and phase responses were determined a number of times, changing the noise/signal ratio in each case. The average percentage errors of each method, as a function of this ratio, are shown in figures 2.1 and 2.2.

From these figures, it is apparent that all these methods

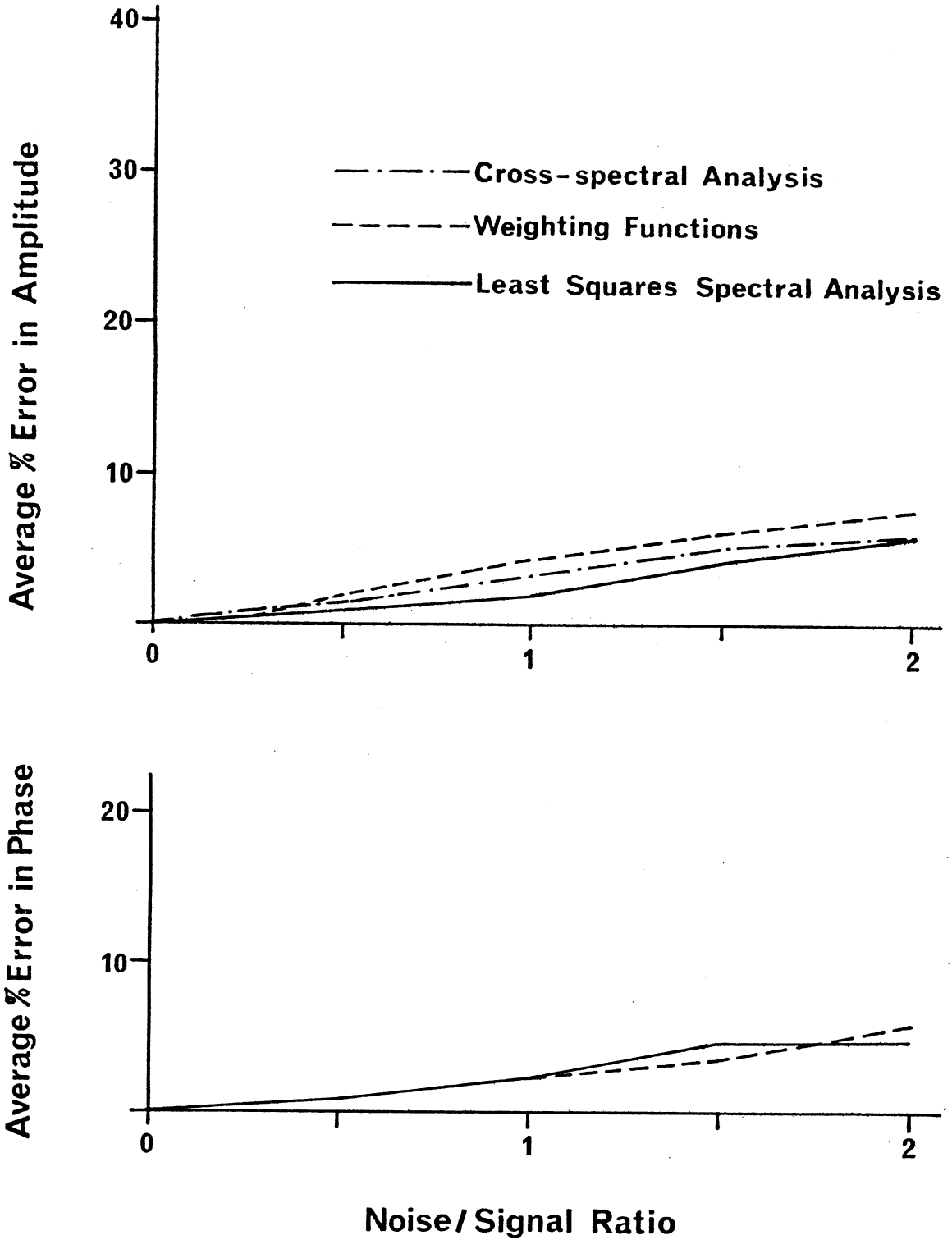

Figure 2.1. Error in Response Methods - Noise on Output only.

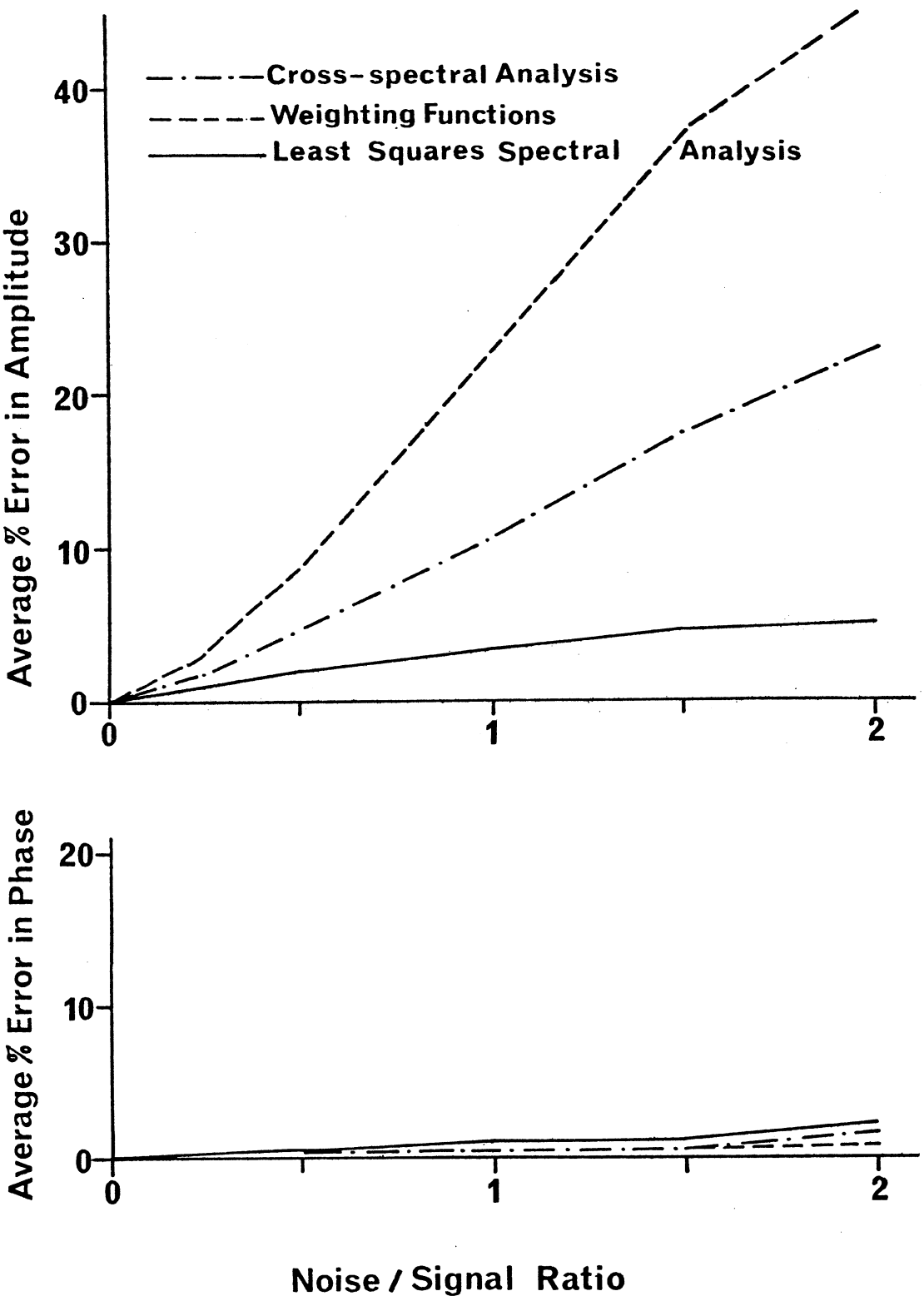

Figure 2.2. Error in Response Methods - Noise on Input and Output

perform equally well in the absence of noise, and also when there is noise in the output series only. This second case is one which does occur in practice, where the input function is exactly known. For example, Munk and Cartwright (1966) use, as input, the known gravitational potential of the sun and moon, and, as output, the noisy sea level series.

Where noise occurs in both input and output, then the results for the three methods diverge rapidly with increasing noise levels. The weighting function approach appears most sensitive to the influence of noise on the input. The divergence between this method and that of cross-spectral analysis is somewhat surprising, as, in the limit, they just represent the time and frequency domain representations of the same technique (Munk and Cartwright, 1966). It is possible that, should the number of lags be increased by a large amount, the results would converge. However, both these methods still produce large percentage errors in the amplitude response. This result is not altogether unexpected, as Bendat and Piersol (1971) have shown that $G_{xx}(f)$ becomes positively biased in the presence of noise.

With regard to the least squares response analysis, this technique performs well, even in the situation of large noise/signal ratios for both input and output. This may be explained if one considers that the least squares approximation, implicit in equation (2.23) and applied to both input and output, tends to act as a frequency discriminator, filtering out the different frequency noise. In this case, the estimates for the amplitudes and phases, in both input and output series, will be unbiased.

For the particular situation considered in this report, both input and output series will be noisy (provisional evaluation of the Halifax mean sea level and pressure data indicated that a noise/signal ratio of up to 2.0 could occur). From this limited analysis, it appears that the least squares response analysis should provide the least-biased estimates of the frequency response. Consequently, this method has been selected for subsequent use.

CHAPTER THREE

DATA

This chapter contains a brief descriptions of the data used to evaluate the response of mean sea level to various forcing functions. Data in the Maritime region of Canada had been collected at the University of New Brunswick for an earlier project involving mean sea level (Anderson, 1978), and this data formed the base for this project. In many cases, little further processing of the data was required. However, in the case of the wind stress data extensive additional processing was necessary, and this is described in a separate subsection. All data used in this study is now stored on disc file at the University of New Brunswick Computer Centre. The positions of all sites are indicated in figure 3.1.

3.1 Mean Sea Level

Monthly mean values of sea level at a number of sites in Maritime Canada were available, with the latest values being for December, 1973. Additional data (up to December 1980) were obtained from the Canadian department of Fisheries and Oceans (J. Nasr, personal communication, 1981) and the two sets merged converting from feet to metres where necessary. Both the pre-1974 and post-1974 levels were referred to the same local Chart Datum, with the exception of the levels at Father's Point (Pt. au Père). In this case, both sets of data are referred to the International Great Lakes Datum, 1955. Details of the connections between the local Chart Datums and

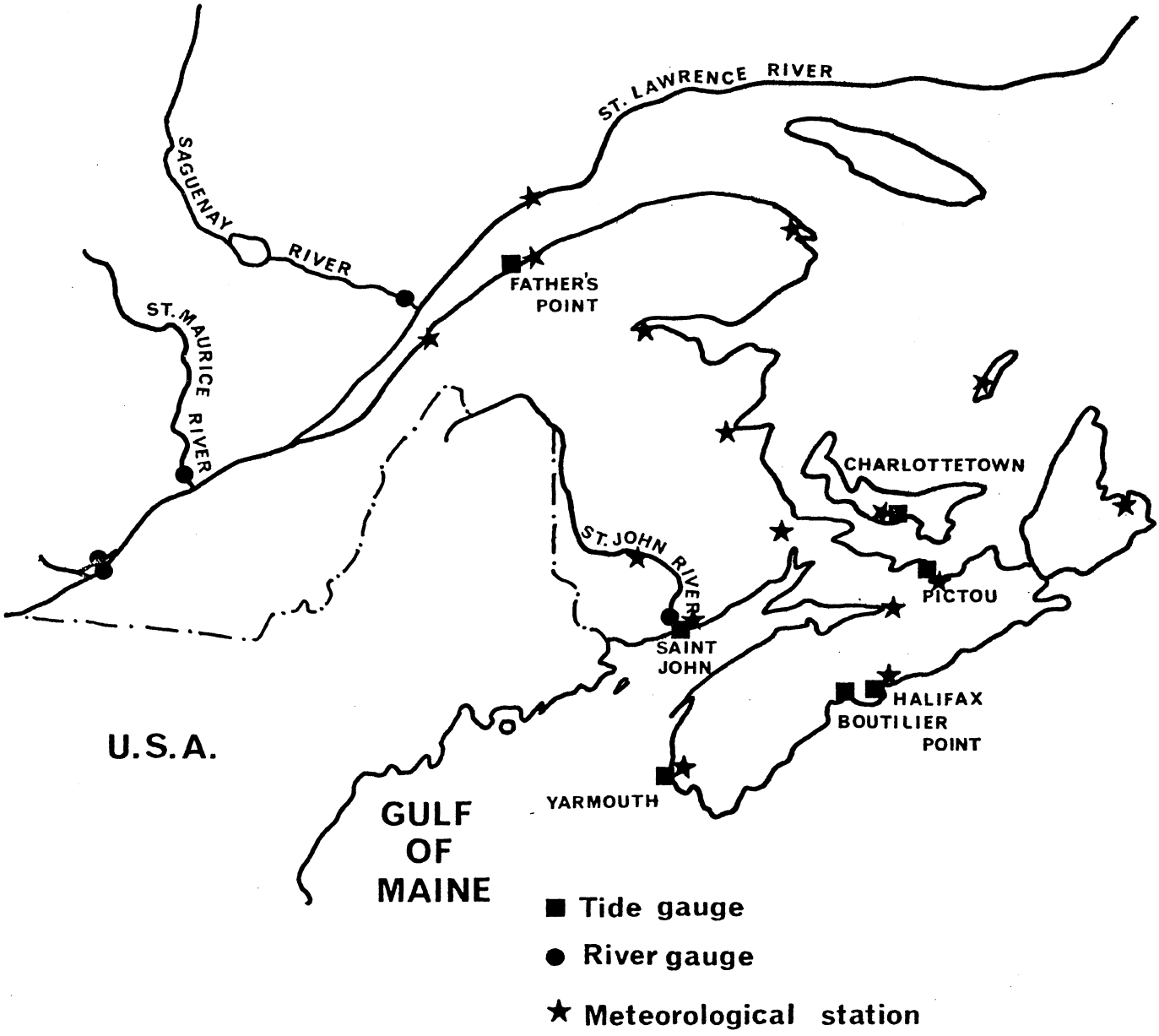

Figure 3.1. Location of Sites in Maritime Canada

the Geodetic Survey of Canada Datum were also provided by the department of Fisheries and Oceans.

Although some levels were available for Pt. Sapin, this gauge was discontinued in 1975, and earlier experiences had suggested that no data at this site could be considered reliable (Vaníček, 1976). Consequently, data from Pt. Sapin were not included in this data set. A summary of the mean sea level data used is given in table 3.1, and the sea levels are depicted graphically in figure 3.2.

3.2 Air Temperature

No water temperature values were available, consequently the rather indirect influence of air temperature had to be considered. Monthly mean air temperature values were available at sites close to the tide gauges described in the previous section, for the months up to December 1973. Post-1973 values were abstracted from the publication Monthly Record provided by Environment Canada, Fredericton. It proved impossible to identify positively the sites used for the pre-1974 data, and consequently it is probable that the two data sets were not recorded at the same sites, resulting in a datum bias. Other datum biases may occur when a site is moved. This is generally accompanied by a change in station number, and a number of changes were identified in this manner. In order to make the data consistent, all pre-1974 values were converted from degrees Fahrenheit to degrees centigrade. A summary of the temperature data is given in table 3.2.

SITE	STATION LOCATION ϕ(°N)	λ(°W)	SPAN OF THE TIME SERIES	SIGNIFICANT GAPS	NUMBER OF AVAILABLE MONTHLY MEAN VALUES	
					Change of datum	
Halifax	44,66	63,59	Oct.1919-Dec.1980	none	none	733
Father's Pt. (Pt. au Père)	48,52	68,47	Jan.1923-Oct.1980	Jan.1932-Dec.1936 Aug.1953-Dec.1955	none	547
Saint John	45,27	66.06	Jan.1927-Dec.1979	Jan.1935-Dec.1938	none	545
Charlottetown	46,23	63,12	Jan.1938-Dec.1980	Nov.1978-Feb.1979	none	496
Yarmouth	43,84	66,12	Aug.1966-July.1980	July 1976-Oct.1976	none	159
Pictou	45,68	62,70	June1965-Dec.1980	Jan.1978-Apr.1978	none	166
Boutilier Pt.	44,66	63,96	Jan.1968-Dec.1980	none	none	152

Table 3.1: Summary of Mean Sea Level Data

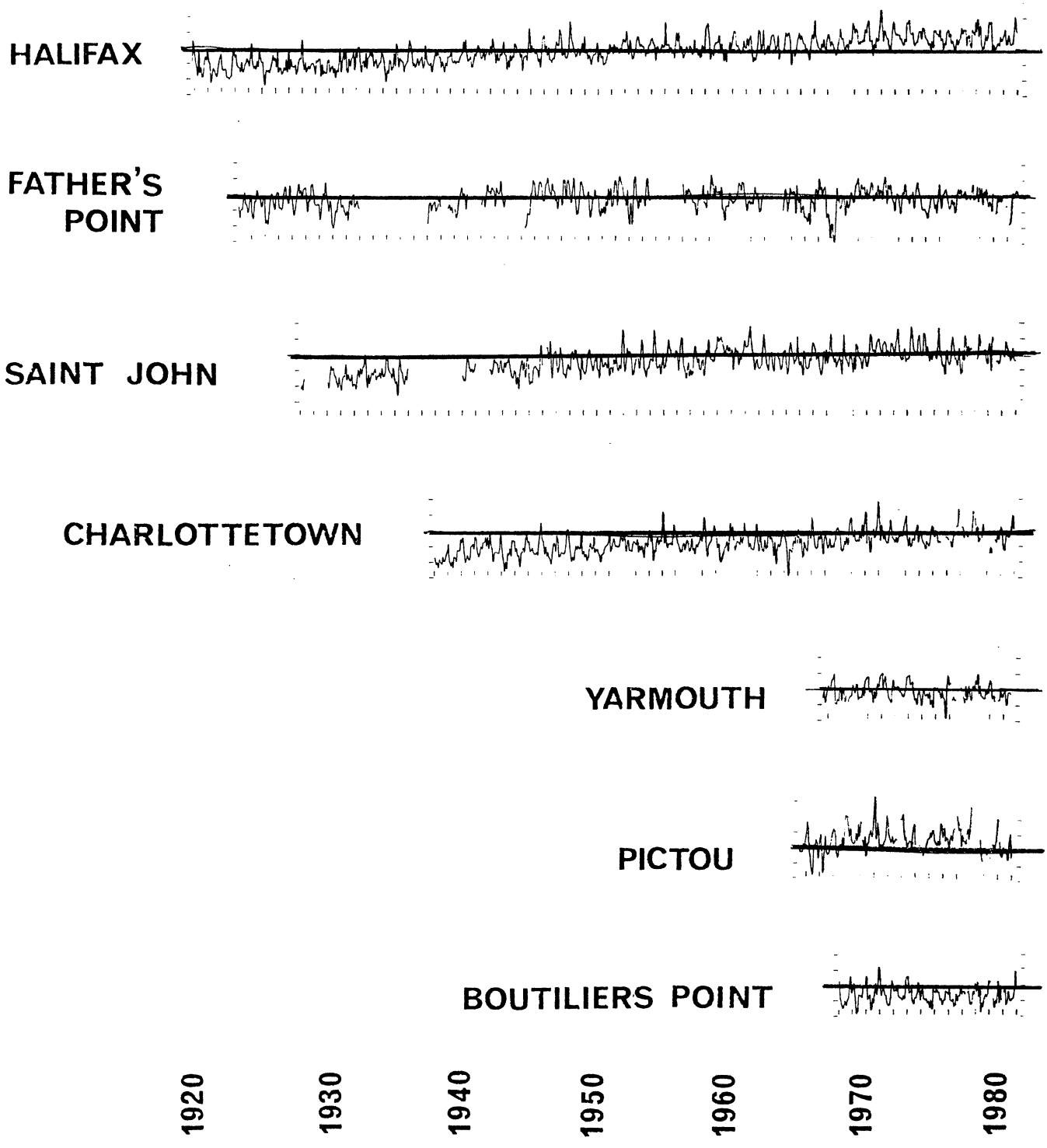

Figure 3.2. Mean Sea Level Time series (divisions on vertical scale represent 10 cm).

SITE	STATION LOCATION ϕ(°N)	λ(°W)	SPAN OF THE TIME SERIES	SIGNIFICANT GAPS	NUMBER OF AVAILABLE MONTHLY MEAN VALUES	
					Change of datum	
Halifax (also for Boutilier Pt.)	44,65	63,57	Jan.1919-Apr.1980	Aug.1933-Sept1939	Oct. 1939 Jan. 1974	662
Father's Pt.	48,50	68,47	Jan.1923-Apr.1980	Jan.1932-Dec.1962 Aug.1951-June1957	Jan. 1974	500
St. John	45,27	66,08	Jan.1927-Apr.1980	Sept1962-July1966	Jan. 1971 Jan. 1974	584
Charlottetown	46,28	63,13	Apr.1943-Apr.1980	Aug.1945-Dec.1945	Jan. 1974	436
Yarmouth	43,83	66,08	Jan.1967-Apr.1980	None	Jan. 1974	158
Stellerton (for Pictou)	45,57	62,65	Jan.1966-Dec.1976	None	Jan. 1974	132

Table 3.2: Summary of Air Temperature Data

3.3 Atmospheric Pressure

As with the air temperature, monthly mean pressure values were available at sites close to the tide gauges. When attempting to reconcile this data with post-1973 values abstracted from the Monthly Record, it was found that no attempt at consistency had been made with the original data. Part of the data set reflected station pressures, part pressures reduced to sea level, and part station pressures reduced to their equivalent values at 0°C. Most of this old data have been replaced, and all pressure data are now in units of millibars, reduced to sea level. As with the temperature data, a number of datum biases have occurred, due to relocation of the observing station. A summary of this data is given in table 3.3

SITE	STATION LOCATION ϕ(°N)	λ(°W)	SPAN OF THE TIME SERIES	SIGNIFICANT GAPS	NUMBER OF AVAILABLE MONTHLY MEAN VALUES	
					Change of datum	
Shearwater (for Halifax & Boutilier Pt.)	44,63	63,50	Nov.1919-Apr.1980	Aug.1936-Dec.1939	Jan. 1940 Jan. 1953	686
Mt. Joli (for Father's Pt.)	48,60	68,20	Jan.1923-Apr.1980	Jan.1932-Dec.1936	Jan. 1943	602
St. John	45,27	66,08	Feb.1919-Apr.1980	Aug.1936-Dec.1939	Jan. 1927 Jan. 1953	678
Charlotte-town	46,28	63,13	Apr.1943-Apr.1980	Aug.1945-Dec.1945	None	439
Yarmouth	43,83	66,08	Jan.1935-Apr.1980	None	Jan. 1944	542
Truro (for Pic-tou)	45,37	63,27	Oct.1960-Apr.1980	None	None	227

Table 3.3: Summary of Atmospheric Pressure Data

In addition to the pressure data at sites near to tide gauges, pressure data has been collected at a number of additional sites, distributed throughout Maritime Canada. This data has been obtained for the purpose of predicting geostrophic winds (described in section 3.5). The positions of all pressure data sites are indicated in figure 3.1.

3.4 River Discharge

River discharge data at a number of sites were available, up to December, 1973. No attempt was made to update this information, as long-period records were available in all cases. At most tide gauge sites the river discharge effect is insignificant. However, there are two exceptions - Saint John, and Father's Point. For Saint John, a single measuring site, just upstream from the tide gauge was available, on the Saint John River. For Father's Point, on the Gulf of St. Lawrence, data from four sites were available. Two of these, on either side of the Montreal Island, effectively monitor all flow in the St. Lawrence river at Montreal. The remaining discharge gauges were on the major downstream tributaries, the St. Maurice and Saguenay rivers. Spectral analysis of the river discharge time series at these four gauges revealed no major differences (except for some phase shifts), and the four series were combined into one. No other changes were made to the data, other than to convert from cubic feet per second to cubic metres per second. A summary of the river discharge data is given in table 3.4.

3.5 Wind Stress

Wind values at the tide gauge sites were not available in any form at the start of this project. This section describes the techniques

SITE	STATION LOCATION φ(°N)	λ(°W)	SPAN OF THE TIME SERIES	SIGNIFICANT GAPS	NUMBER OF AVAILABLE MONTHLY MEAN VALUES	
					Change of datum	
La Salle (for Father's Pt.)	45,42	73,62	Jan.1923-Oct.1973	Jan.1932-Dec.1936	none	468
des Prairies (for Father's Pt.)	45,53	73,72	Jan.1923-Oct.1973	Jan.1932-Dec.1936 Aug.1953-Dec.1955	none	468
Saguenay (for Father's Pt.)	not known		Jan.1923-Oct.1973	Jan.1932-Dec.1936 Aug.1953-Dec.1955	none	468
St. Maurice (for Father's Pt.)	not known		Jan.1923-Oct.1973	Jan.1932-Dec.1936 Aug.1953-Dec.1955	none none	468
Saint John	45,28	66,09	Jan.1927-Dec.1973	none	none	560
Middle (for Pictou)	45,50	62,78	Jan.1966-Dec.1973	none	none	96

Table 3.4: Summary of River Discharge Data

used to compute the wind stress from wind and pressure data. Two different sets of wind data were obtained. The first of these consisted of a set of hourly wind velocities at four Maritime cities, supplied by Environment Canada (M.S. Webb, personal communication, 1981). The second is a set of modelled wind velocities, determined from pressure gradients.

3.5.1 Observed Wind

This subsection describes the procedures used to convert the hourly wind velocities, obtained from Environment Canada, to monthly mean components of wind velocity. The data tape supplied contains the hourly values of a number of meteorological parameters for sites at Fredericton, Saint John, Charlottetown, and Shearwater (Halifax). These data cover the period January 1953 to December 1979. For each day, the wind data are contained in two records, the one containing hourly wind speed values, the other hourly wind direction values, using a 18-sector code (36 sectors after 1971).

The first processing steps involved abstracting the wind data and then computing the North and East components of the wind vector for each hour (in units of m/sec.). Note that the meteorologists convention is used here - a positive North component imples a wind from the North. Subsequent steps involved computing daily mean and then monthly mean North and East components. Where less than 18 hourly values were available for any one day, no daily mean was computed. Where less than 20 daily mean values were available for any one month, no monthly mean was computed.

3.5.2 Modelled Wind

Wind modelling was carried out in two steps. Firstly, the geostrophic wind was computed using mean pressure gradients. Then this wind was used, together with the observed wind of the previous section, to determine a mean scale factor and rotation to be applied to all geostrophic winds in the region. The steps are as follows. The equation for the geostrophic wind is given by (Petterssen, 1969):

$$V = \frac{1}{Pf} \frac{\partial P}{\partial s} \quad , \tag{3.1}$$

where $\frac{\partial P}{\partial s}$ is the horizontal pressure gradient, P is the density of air (a value of 0,0012 gm cm^{-3} was assumed), and f is the Corilis parameter, given by:

$$f = 2\omega \sin \phi \quad . \tag{3.2}$$

Here, ϕ is the latitude of the point, and ω is the angular velocity of the rotation of the earth ($\omega = 7{,}272*10^{-5}\ s^{-1}$).

Where a North component and a East component are desired, (3.1) can be rewritten as:

$$V_N = - \frac{1}{2P\omega \sin \phi} \frac{\partial P}{\partial x} \quad ,$$

$$V_E = \frac{1}{2P\omega \sin \phi} \frac{\partial P}{\partial y} \quad , \tag{3.3}$$

where (x,y) is a local coordinate system with its x axis directed towards the East, and y axis directed towards the North.

Before the geostrophic wind can be computed, the terms $\frac{\partial P}{\partial x}$, $\frac{\partial P}{\partial y}$ which represent the gradients must be evaluated, Making use of the pressure time series described in section 3.3, we can write

$$P = P(\phi, \lambda, t)$$

or using a local coordinate system:

$$P = P(x,y,t),$$

where: $$x = (\lambda-\lambda_o)\ R \cos \phi_o,$$

$$y = (\phi-\phi_o)\ R \quad ,$$

and R is the mean radius of the earth (R ≐ 6371 km), and (ϕ_o,λ_o) is an arbitrarily chosen local origin. At each instant of time, t, the pressure field can be modelled by a low-order algebraic polynomial:

$$P_t(x,y) = \sum_{\substack{i=0 \\ j=0}}^{n} a_{ij}\, x^i\, y^i \,. \tag{3.4}$$

The coefficients, a_{ij}, can be found by applying the least-squares technique to equation (3.4), yielding a solvable set of normal equations:

$$\sum_{\substack{k=0 \\ \ell=0}}^{n} \langle x^i y^i,\ x^k y^\ell \rangle \cdot a_{k\ell} = \langle x^i y^i,\ P_t \rangle \quad \begin{matrix} i=0,\ldots n \\ j=0,\ldots n \end{matrix}, \tag{3.5}$$

Once the coefficients, a_{ij} are known, the horizontal gradients of pressure, at a selected instant t of time, are given by:

$$\frac{\partial P_t}{\partial x} = \sum_{\substack{i=1 \\ j=0}}^{n} i a_{ij}\, x^{i-1} y^j \,;$$

$$\frac{\partial P_t}{\partial y} = \sum_{\substack{i=0 \\ j=0}}^{n} j a_{ij}\, x^i y^{j-1} \,. \tag{3.6}$$

Monthly mean sea level pressure values at 15 sites distributed across the Maritimes were acquired, and could be used for estimating the coefficients a_{ij}. However, due to gaps in the data, as few as 8 points were available at any one time, and it proved impossible to

reliably model the pressure field for dates prior to 1953. Both first- and second-order polynomials were evaluated for use in equation (3.5). The first-order (4 coefficients) provided smoother values of the pressure gradients and was chosen for subsequent use.

The geostrophic wind, as determined does not take into account the effects of friction and topographic modification, and must be considered as only a first approximation to the real wind. The observed wind data described in subsection 3.5.2 was used to further improve the geostrophic wind. At each of the four sites a determination was made of the rotation and scale factor relating the observed and goestrophic winds. For this purpose, the mean wind vector for each month can be represented by its speed $|V|$, and direction, α:

$$\begin{aligned} |V| &= (V_N^2 + V_E^2)^{\frac{1}{2}} \quad , \\ \alpha &= \arctan \frac{V_E}{V_N} \quad . \end{aligned} \tag{3.7}$$

The temporal mean rotation and scale between the observed and geostrophic winds at each site is then given by:

$$\begin{aligned} \theta &= \frac{1}{n} \sum_{i=1}^{n} (\alpha_{obs} - \alpha_{geos})_i \quad , \\ \kappa &= \frac{1}{n} \sum_{i=1}^{n} \left(\frac{|V|_{obs}}{|V|_{geos}}\right)_i \quad , \end{aligned} \tag{3.8}$$

where the subscript i denotes that the appropriate values are determined at each t_i ($t = 1,\ldots,n$). Values of θ, and κ were determined at each of the four sites. The mean rotation and scale factor (of -22°,4 and 0,35 respectively) were applied to all the geostrophic wind data at the four sites, resulting in an RMS error for a single monthly mean wind vector of 32° in direction and 0,6 m/sec in speed.

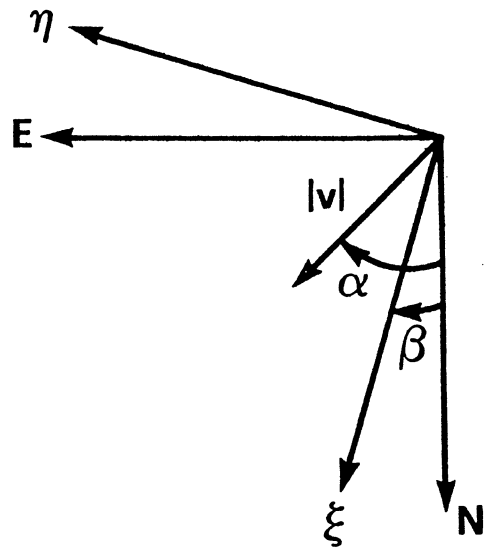

Figure 3.3a. Rotation of Wind Coordinate System

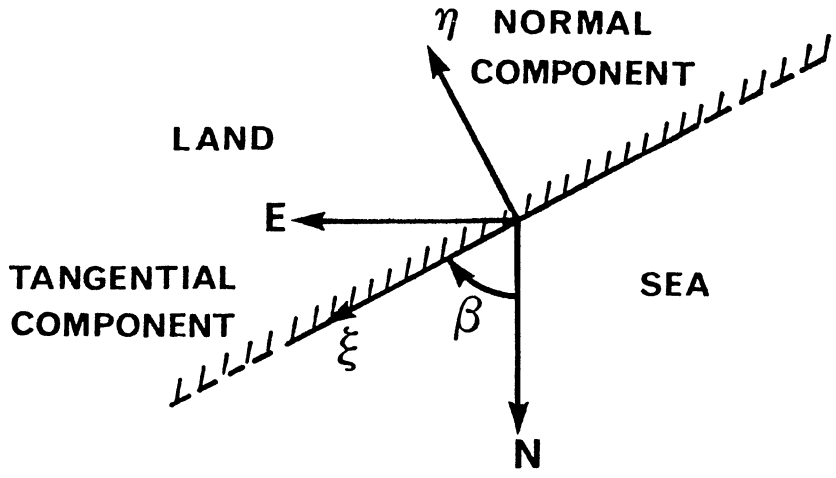

Figure 3.3b. Orientation Convention for Wind Stress Components

The rotation of -22°,4 is in accordance with what may be expected (Peterssen, 1969), but the scale factor appears to be somewhat on the low side. The scale factor is normally considered to lie between 0,4 and 0,7.

3.5.3. Wind Stress

The driving force acting on the sea surface is not the wind, but the wind stress. Consequently, the final step in the preparation of the necessary data for determining the sea level response, is to calculate the wind stress in two orthogonal directions (not necessarily the North-South, East-West directions). This operation is carried out in two steps. Firstly the coordinate system is rotated to the desired orientation, then the wind stress components are calculated. In Figure 3.3a, both the original and rotated coordinate system are indicated. The wind vector, with speed $|V|$ and direction α in the original system, has components V_ξ , V_η in the new system:

$$\begin{aligned} V_\xi &= |V| \cos(\alpha - \beta) \\ V_\eta &= |V| \sin(\alpha - \beta) \end{aligned} \quad , \tag{3.9}$$

The wind stress components are given by (Willebrand, 1978):

$$\begin{aligned} \gamma_\xi &= C\rho\, |V| \cdot |V| \cos(\alpha-\beta) \\ \gamma_\eta &= C\rho\, |V| \cdot |V| \sin(\alpha-\beta) \end{aligned} \quad , \tag{3.10}$$

or:

$$\begin{aligned} \gamma_\xi &= C\rho\, |V| \cdot V_\xi \\ \gamma_\eta &= C\rho\, |V| \cdot V_\eta \end{aligned} \quad , \tag{3.11}$$

where ρ is the density of air (ρ = 0,0012 gm cm^{-3}) and C is drag coefficient. Various models for the drag coefficient have been proposed, including one

in which the drag coefficient is itself a linear function of wind speed (Smith and Burke, 1975). However, considering the low mean wind velocities used here, an average value of $1,5 * 10^{-3}$ appears adequate.

In the formulation set up above, it is possible to compute the wind stress components at an arbitrary orientation. Two orientations that could be used are those of a North-East coordinate system (i.e. $\beta = 0$) or one aligned with an axis perpendicular to the coast. The second alternative appears to be the more physically meaningful and has been used in this synthesis. The orientation convention adopted is that indicated in figure 3.3b, in which the η-axis is directed from the sea towards the land, and ξ-axis is directed to form a left-handed coordinate system. At each tide gauge site the normal (to the coastline) and tangential wind stress components have been computed for each of two following cases. In the first instance, the orientation of the coastline has been established regionally (i.e., using the trend of the coastline over several hundred kilometres), and in the other instance, locally (using the local coastline features within a few kilometres of the tide gauge site).

The wind data used to establish these wind stress data sets have been the modelled wind (i.e. geostrophic wind rotated by -22°,4 and scaled by 0,35). Although observed wind data is available near three tide guage sites, this data has not been used, as it may be considerably modified by the local topography at the meteorological station, which may be some distance from the tide gauge site. It is felt that the modelled wind may better represent the regional characteristics of the wind. A summary of the wind data used is given in table 3.5.

SITE	STATION LOCATION φ(°N)	λ(°W)	SPAN OF THE TIME SERIES	SIGNIFICANT GAPS	NUMBER OF AVAILABLE MONTHLY MEAN VALUE	
					Change of datum	
Halifax	44,66	63,59	Jan.1953-Dec.1979	none	none	324
Father's Pt.	48,52	68,47	Jan.1953-Dec.1979	none	none	324
Saint John	45,27	66,06	Jan.1953-Dec.1979	none	none	324
Charlottetown	46,23	63,12	Jan.1953-Dec.1979	none	none	324
Yarmouth	43,84	66,12	Jan.1953-Dec.1979	none	none	324
Pictou	45,68	62,70	Jan.1953-Dec.1979	none	none	324
Boutilier Pt.	44,66	63,96	Jan.1953-Dec.1979	none	none	324

Table 3.5: Summary of Generated Wind Data

CHAPTER FOUR

APPLICATION AND RESULTS

4.1 Practical Application of the Least Squares Response Method

The least squares technique has been applied to mean sea level (tide gauge) and meteorological data from the Maritime region of Canada. Software, developed by Steeves (1981a) for application on a similar problem concerning earth tide tilt, was used, with minor modifications to the input and output structure.

The computer programs cannot be used indiscriminatly, and a certain amount of subjective decision-making is involved. To aid those who may wish to use this approach, the steps involved in determing the frequency response function are described in some detail in the next four paragraphs.

For each input series involved (at one site, these may be: pressure, temperature, river discharge, normal wind stress, tangential wind stress), a number of passes of the data would be made through the main computer program, SPANER. (For details concerning SPANER, refer to Steeves, 1981a). In the first of these only the coefficients of datum biases and of a linear trend would be determined, and the data scanned for any obvious blunders or omissions. The spectrum determined in this pass would provide the predominant frequencies to be treated as "systematic noise" (Vaníček, 1971) in subsequent passes. Suppresion of these constituents in this sequential fashion enhances the contribution of weather constituents, without distorting the positions of peaks within the spectrum (Taylor and Hamilton, 1972). As an example,

figure 4.1 shows portions of the spectrum of the air temperature at Halifax, before and after the predominant 12 month constituent is suppressed.

In an attempt to reduce the subjectivity of the selection of predominant peaks, two criteria have been used. The first of these involves a 95% significance test for the spectral peaks (Steeves, 1981c). This statistic is a function of the degrees of freedom of the least squares process, and decreases with increasing length of the time series. The 95% confidence level is indicated in figure 4.1b. A further criterion is that known as Rayleigh's (Godin, 1972), which provides a means of detecting whether two spectral peaks are resolvable (or distinguishable from one another). This criterion is also a function of time series length.

Once the significant constituents have been identified in each input time series, these frequencies can be enforced in a least squares response analysis of the mean sea level data. In addition to the influence of these meteorological inputs, the monthly mean sea levels will be affected by the long periodical gravitational effects. Consequently, these known long periodical constituents are also enforced. The constituents used, with their periods, are given in table 4.1. It is important to note that all these input constituents should be enforced simultaneously, as the response to them will, to some extent, be correlated.

At the same time, however, it is necessary to ensure that all the enforced frequencies are separable, using Rayleigh's criterion, and that no frequencies are duplicated. This means that it is not possible to separate the contributions to mean sea level of different

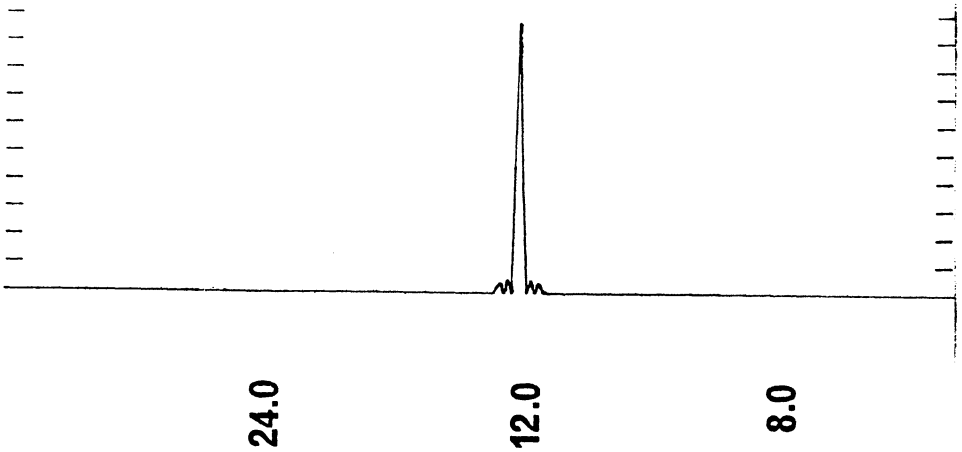

Figure 4.1a: Halifax Air Temperature Spectrum (divisions on vertical scale represent 10% of variance, periods given in months).

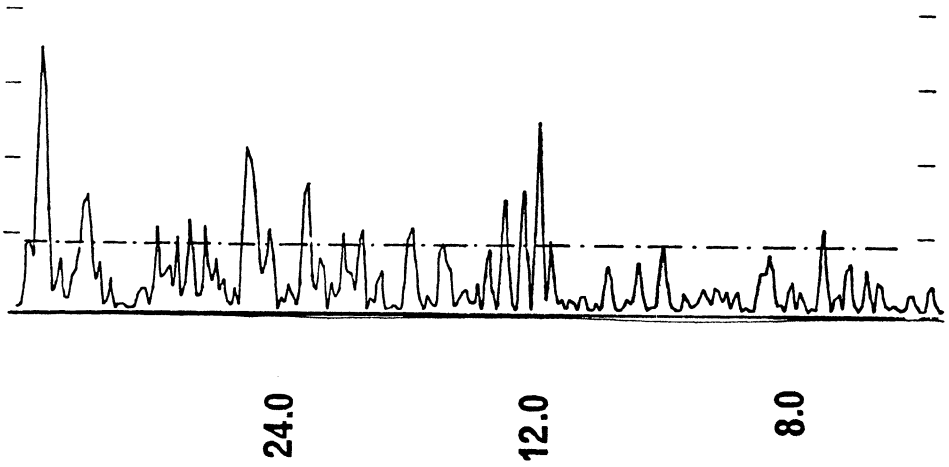

Figure 4.1b: Halifax Air Temperature Spectrum - 12 month period removed (divisions on vertical scale represent 1% of variance periods given in months).

CONSTITUENT	PERIOD
Semi-annual (Ssa)	6 months
Annual (Sa)	12 months
Chandler (pole tide)	14,3 months
Lunar perigee (p)	106,2 months
Lunar nodal (N)	223,4 months

Table 4.1: Long-period Gravitational Constituents

inputs with common frequencies. For example, the 12 month periodicity appears in all the inputs, and the amplitude and phase response determined at this period cannot be separated into its individual components (however, as is discussed later, it is possible to interpolate the individual responses at these common frequencies).

Using the above-described procedure, it was possible to obtain up to twenty amplitude and phase response values for each input series, this number depending upon the length of the series, and the degree of correlation with other input series. Error estimates for each amplitude and phase response were also determined, at the 1σ (67% confidence) level. These estimates were calculated using conventional correlated error propagation through the least squares approximation procedure.

It must be noted that some spurious periods appear in the monthly averages due to an aliasing of diurnal and semidiurnal tidal periods. The power on these periods is, however, insignificant.

4.2 Frequency Response: Results

This section describes the results obtained by the least squares response technique. Each type of input series is discussed in a separate subsection. The technique was applied to a total of seven tide gauge sites in Maritime Canada. However, at only four of these were the series sufficiently long to provide consistent results. At the remaining three (Yarmouth, Pictou, Boutilier Point), the response functions tend to be erratic, with large error bars. So much so that at the end we have decided to leave the Boutilier Point results out altogether. The other two locations are included for comparison.

4.2.1 Atmospheric Pressure

Of the four inputs, response to this parameter appears to be the most consistent (figure 4.2). There is little change throughout the frequency range, and the amplitude response is similar at most sites. The phase response (close to 180°) is what would be expected (inverse barometer effect). The only noticeable departures are at the sites with short time spans of data. The magnitude of the amplitude response is close to the static response of 10 mm per mbar, and is in good agreement with that obtained in other investigations (Hamon, 1966; Wunsch, 1972, Thompson, 1979). However, the magnitude is somewhat larger than that determined in two other investigations for the same region of North America (Vaníček, 1978; Anderson, 1978).

4.2.2 Air Temperature

The response of sea level to air temperature changes is rather tenously linked through the effect of (water) temperature induced density changes. Lack of a reliable heat transfer model for air/sea temperature precluded a more direct approach. Consequently, it had been anticipated that the response would be rather poorly defined, and this proved to be the case. There is a significant scatter in the determined amplitude and phase responses (figure 4.3), with an average value for the amplitude response near 20 mm per degree Centigrade. This response is larger than anticipated, and is significantly larger that that obtained in another investigation (Vaníček, 1978). The interpolated response at the annual cycle would result in a sea level response of the order of 200 mm in amplitude. Such a large response does not appear

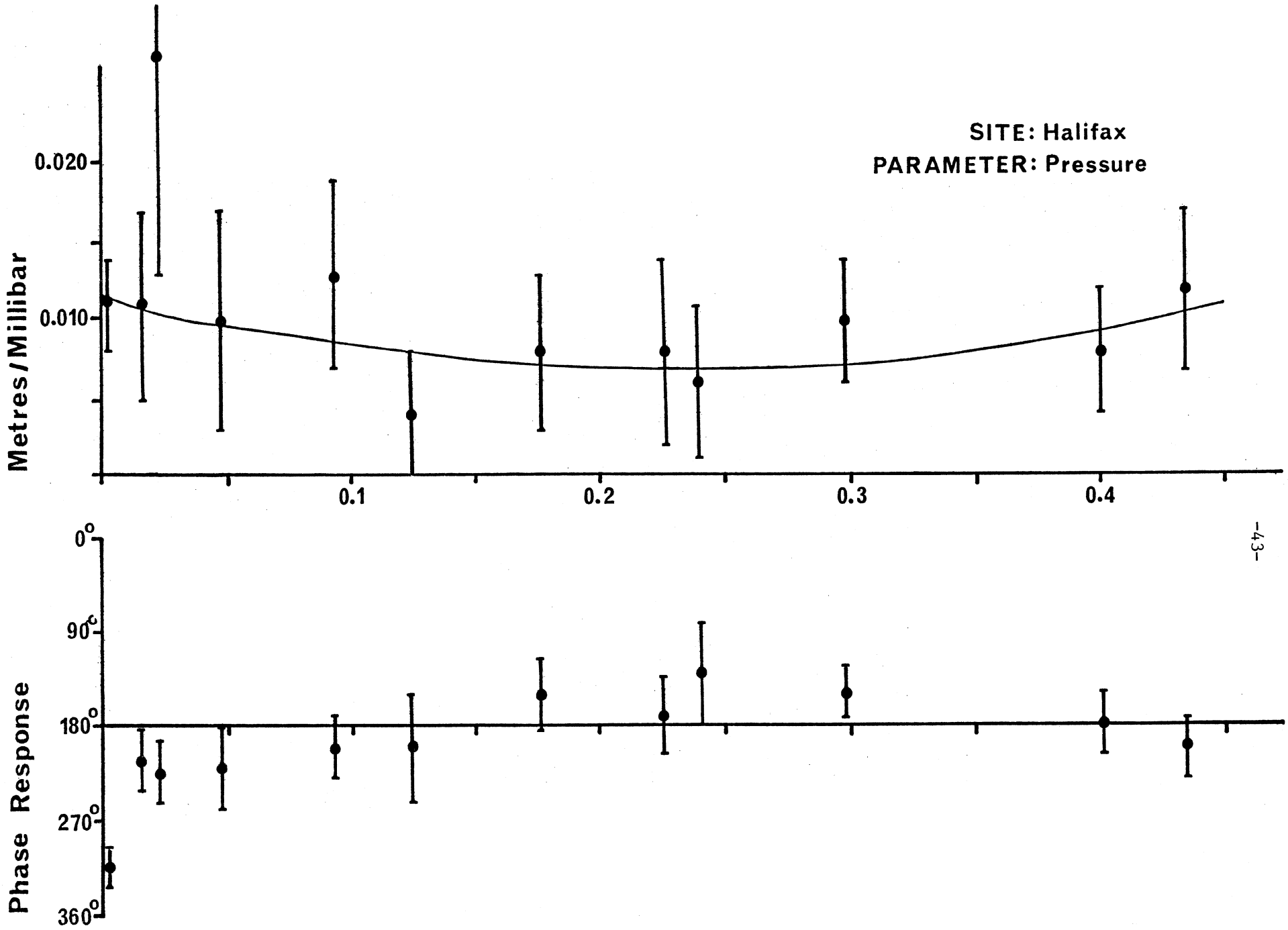
SITE: Halifax
PARAMETER: Pressure
Metres/Millibar
0.020
0.010
0.1
0.2
0.3
0.4
Phase Response
0°
90°
180°
270°
360°
FREQUENCY(cycles per month)

Figure 4.2.

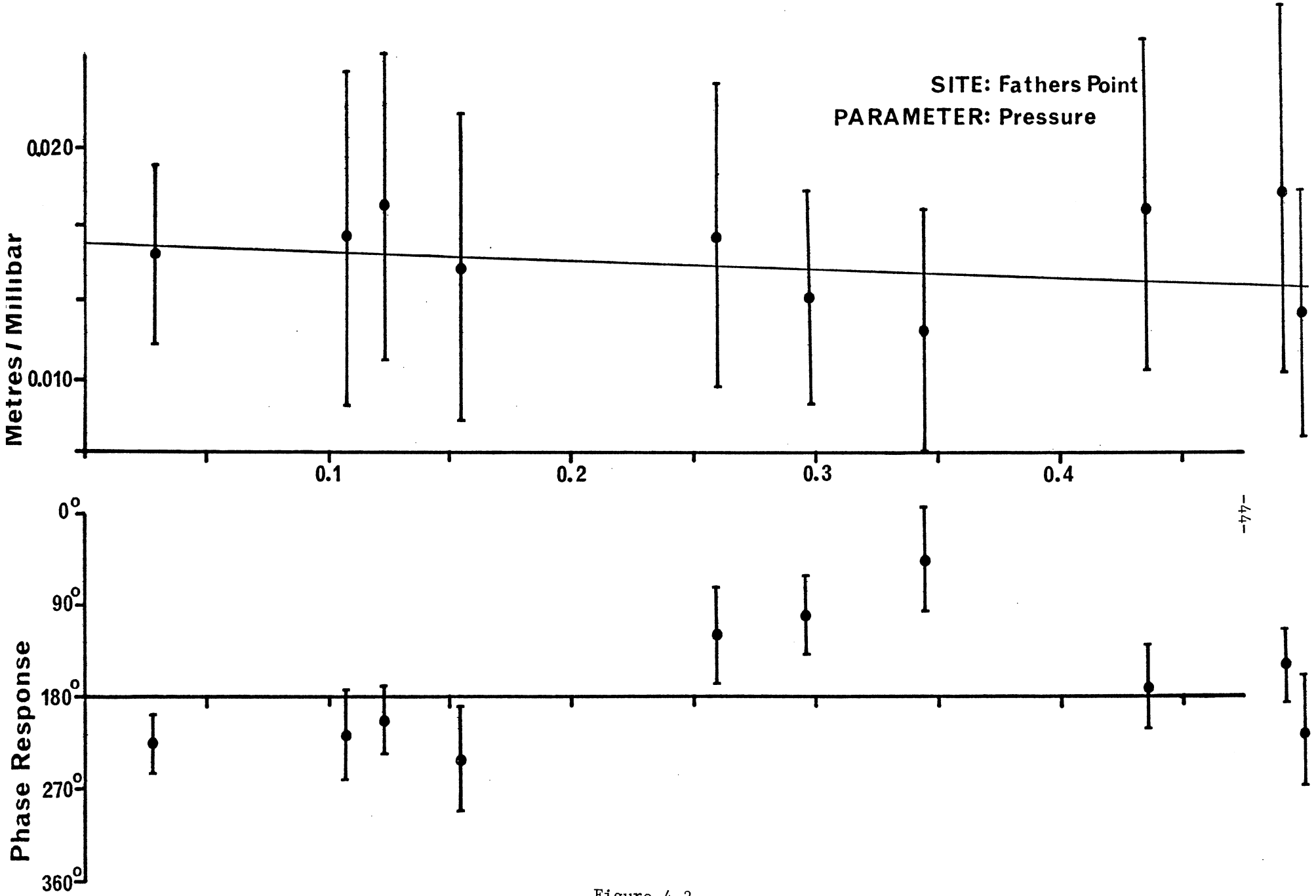
SITE: Fathers Point
PARAMETER: Pressure
Metres / Millibar
0.020
0.010
0.1
0.2
0.3
0.4
Phase Response
0°
90°
180°
270°
360°
FREQUENCY (cycles per month)

Figure 4.2.

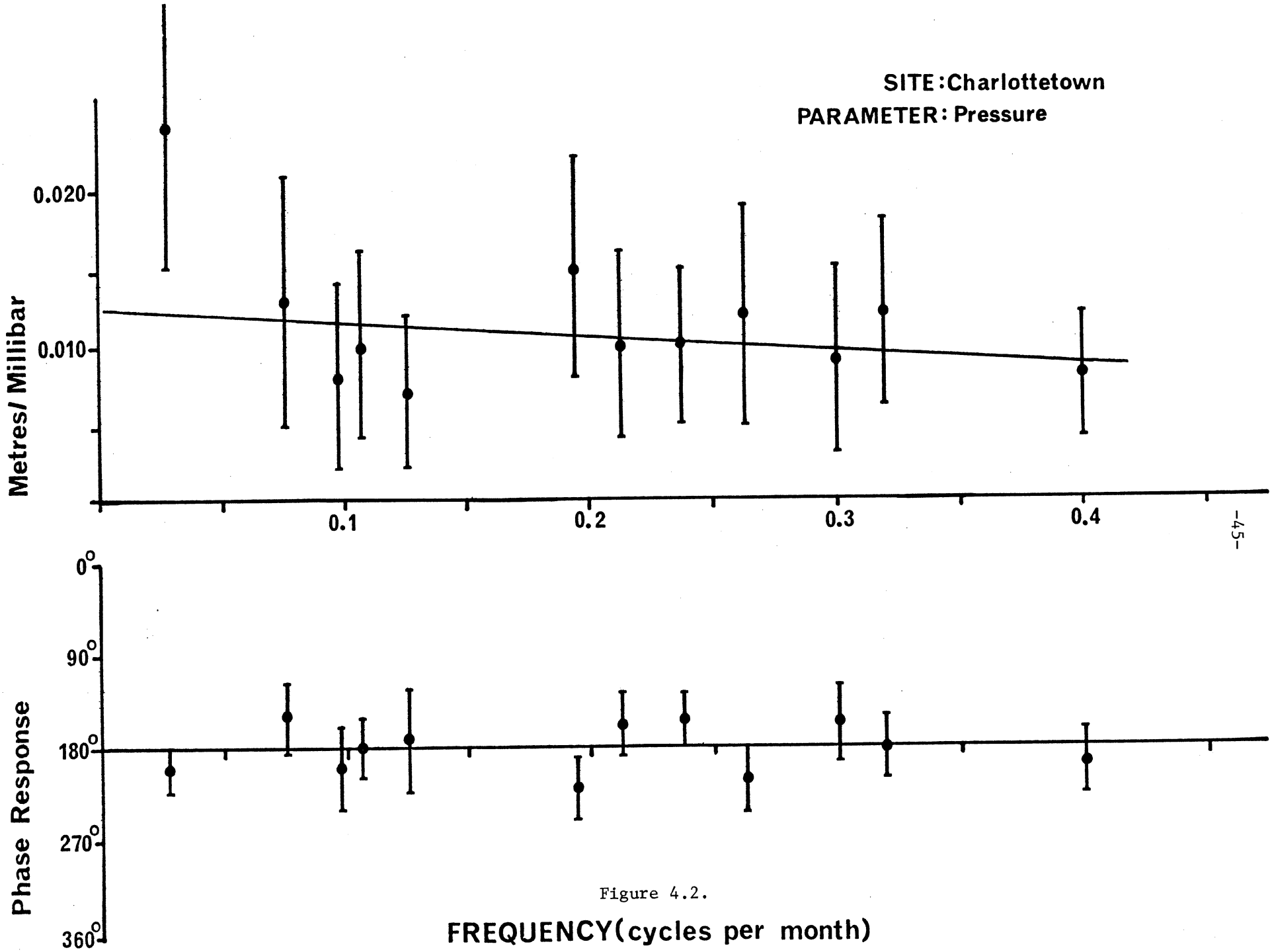
SITE:Charlottetown
PARAMETER: Pressure
Metres/ Millibar
0.020
0.010
0.1
0.2
0.3
0.4
Phase Response
0°
90°
180°
270°
360°
FREQUENCY(cycles per month)

Figure 4.2.

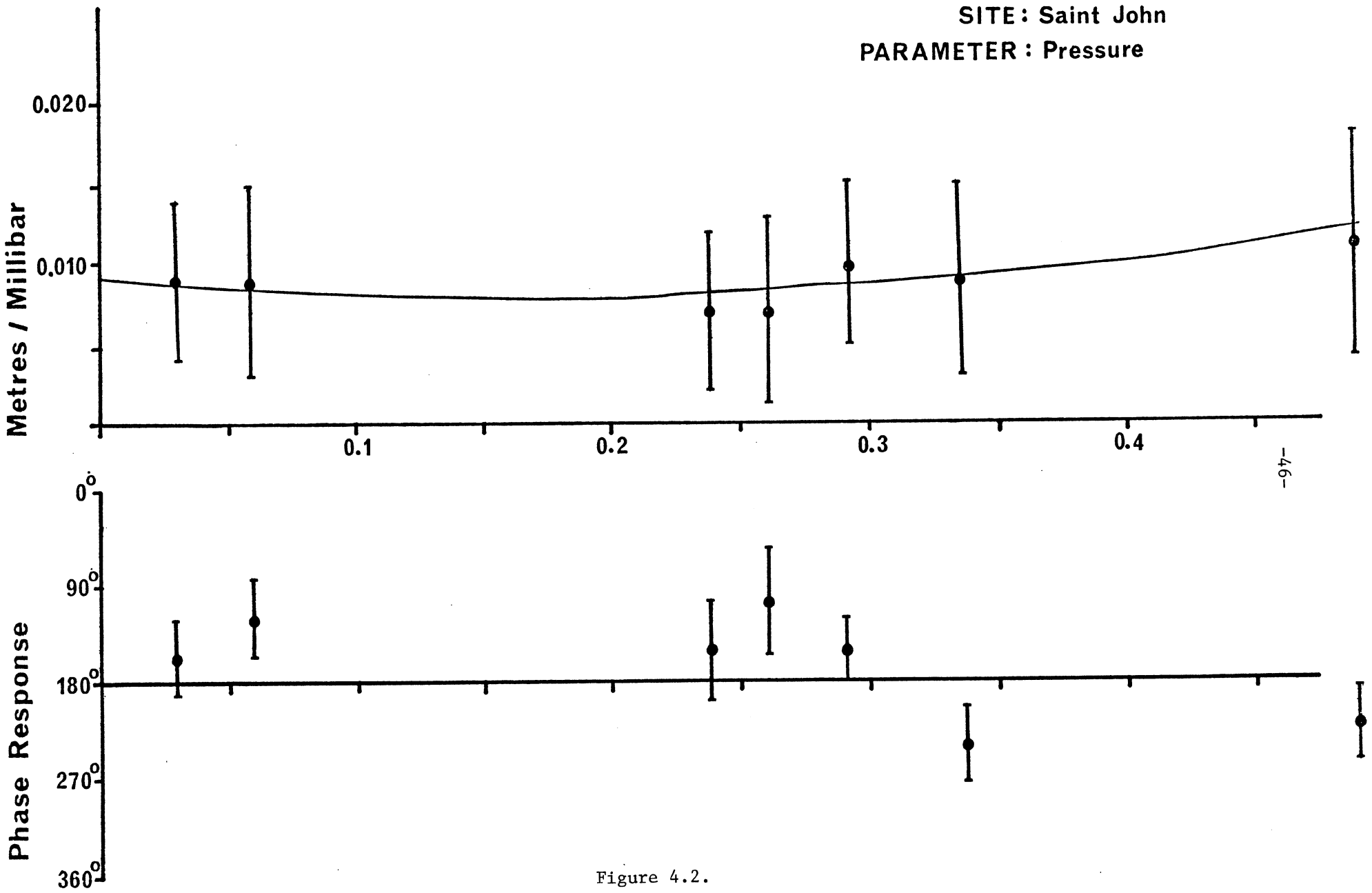
SITE: Saint John
PARAMETER: Pressure
Metres / Millibar
0.020
0.010
0.1
0.2
0.3
0.4
Phase Response
0°
90°
180°
270°
360°
FREQUENCY(cycles per month)

Figure 4.2.

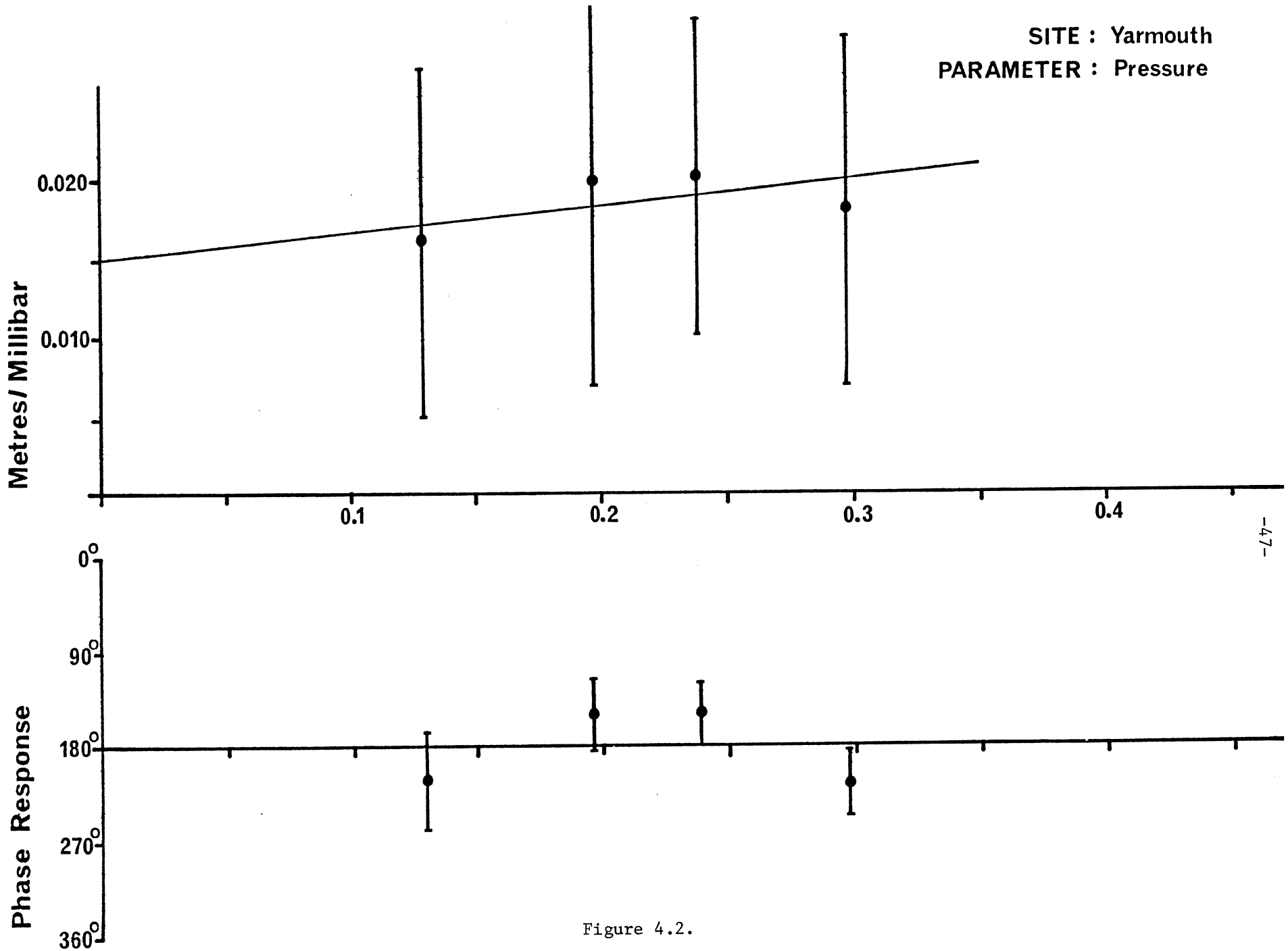
SITE : Yarmouth
PARAMETER : Pressure
Metres/Millibar
0.020
0.010
0.1
0.2
0.3
0.4
Phase Response
0°
90°
180°
270°
360°
FREQUENCY (cycles per month)

Figure 4.2.

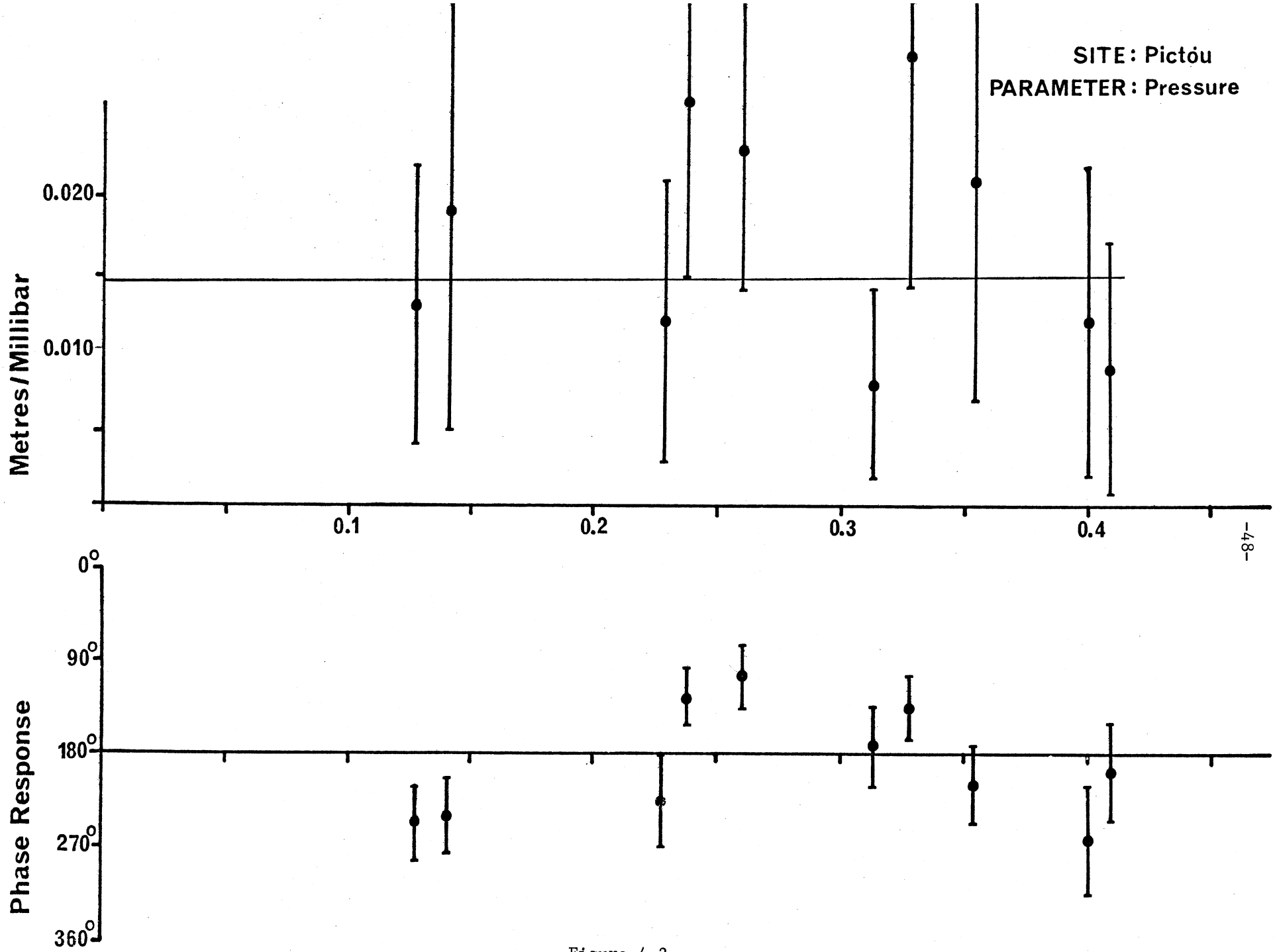
SITE: Pictou
PARAMETER: Pressure
Metres/Millibar
0.020
0.010
0.1
0.2
0.3
0.4
Phase Response
0°
90°
180°
270°
360°
FREQUENCY(cycles per month)

Figure 4.2.

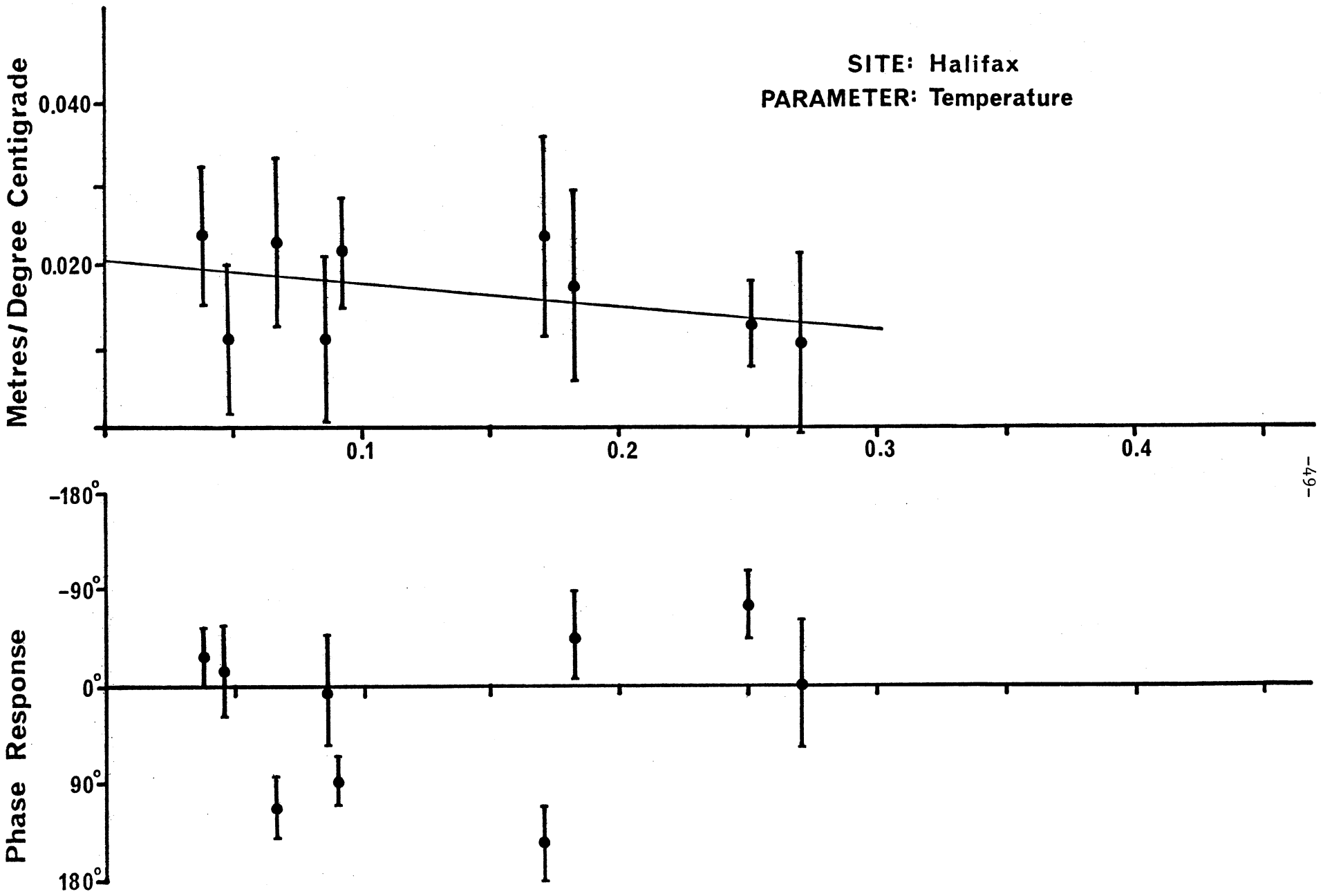
SITE: Halifax
PARAMETER: Temperature
Metres/Degree Centigrade
0.040
0.020
0.1
0.2
0.3
0.4
Phase Response
-180°
-90°
0°
90°
180°
FREQUENCY(cycles per month)

Figure 4.3.

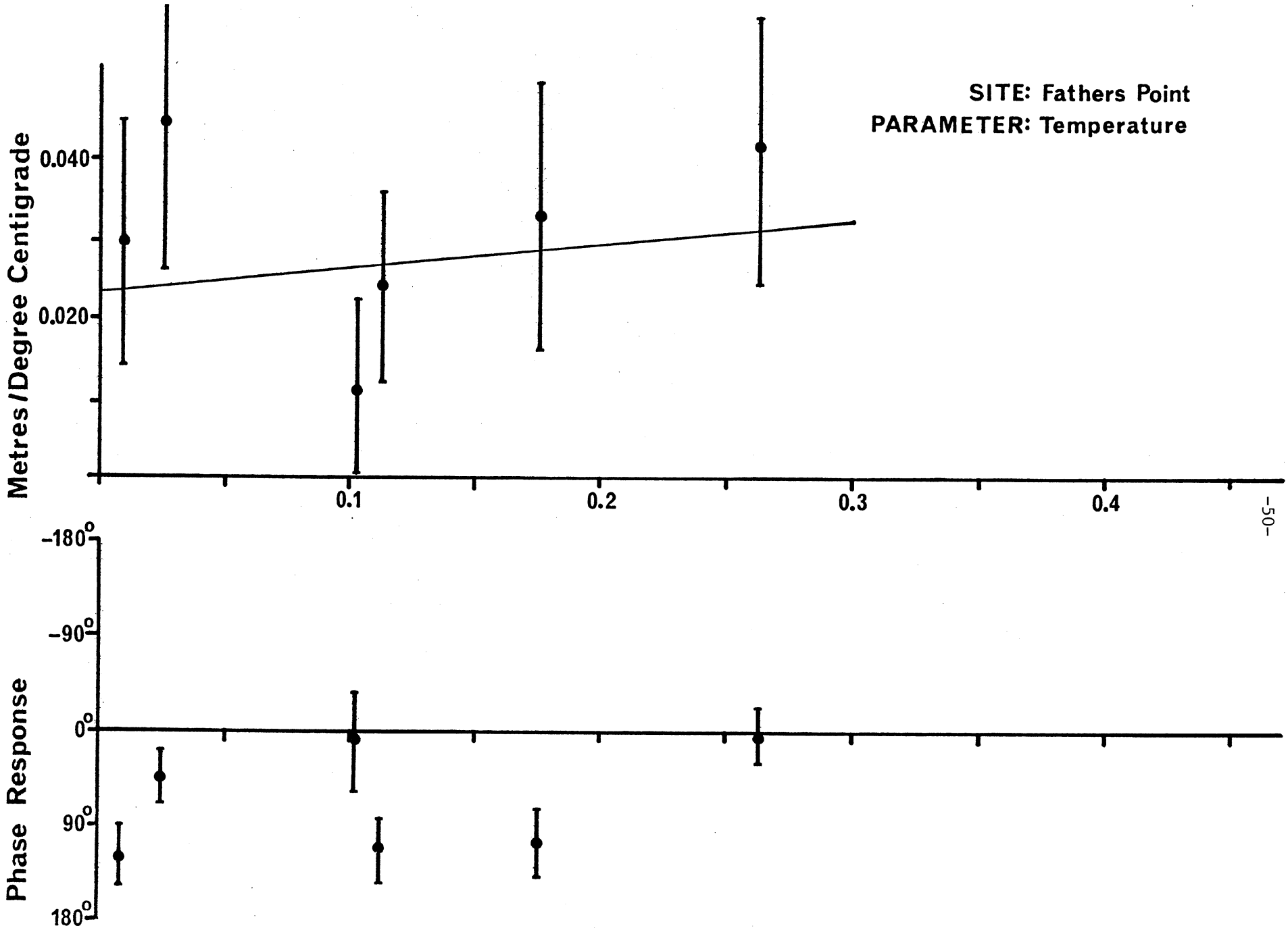
SITE: Fathers Point
PARAMETER: Temperature
Metres/Degree Centigrade
0.040
0.020
0.1
0.2
0.3
0.4
-50-
Phase Response
-180°
-90°
0°
90°
180°
FREQUENCY(cycles per month)

Figure 4.3.

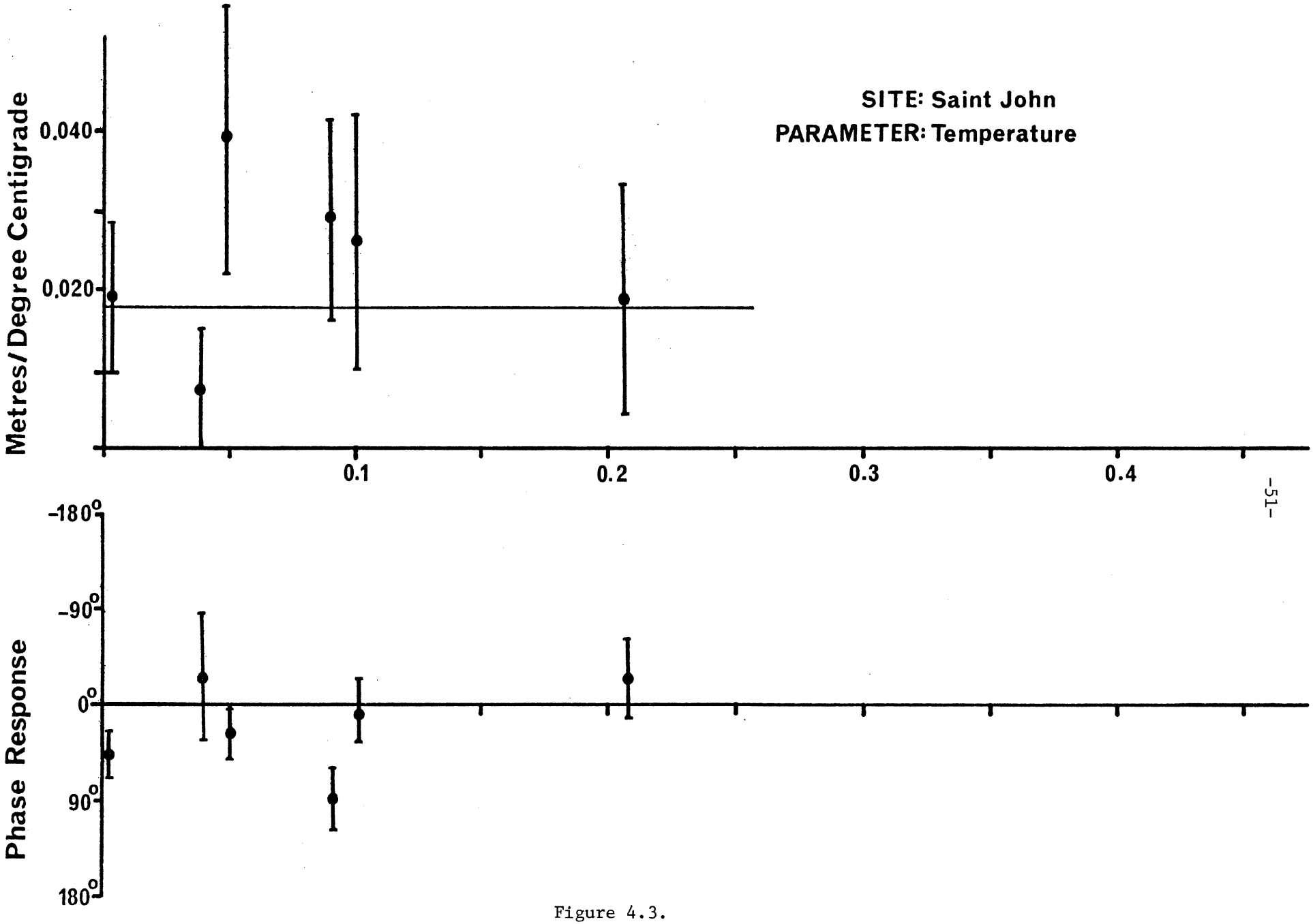
SITE: Saint John
PARAMETER: Temperature
Metres/Degree Centigrade
0.040
0.020
0.1
0.2
0.3
0.4
Phase Response
-180°
-90°
0°
90°
180°
FREQUENCY(cycles per month)

Figure 4.3.

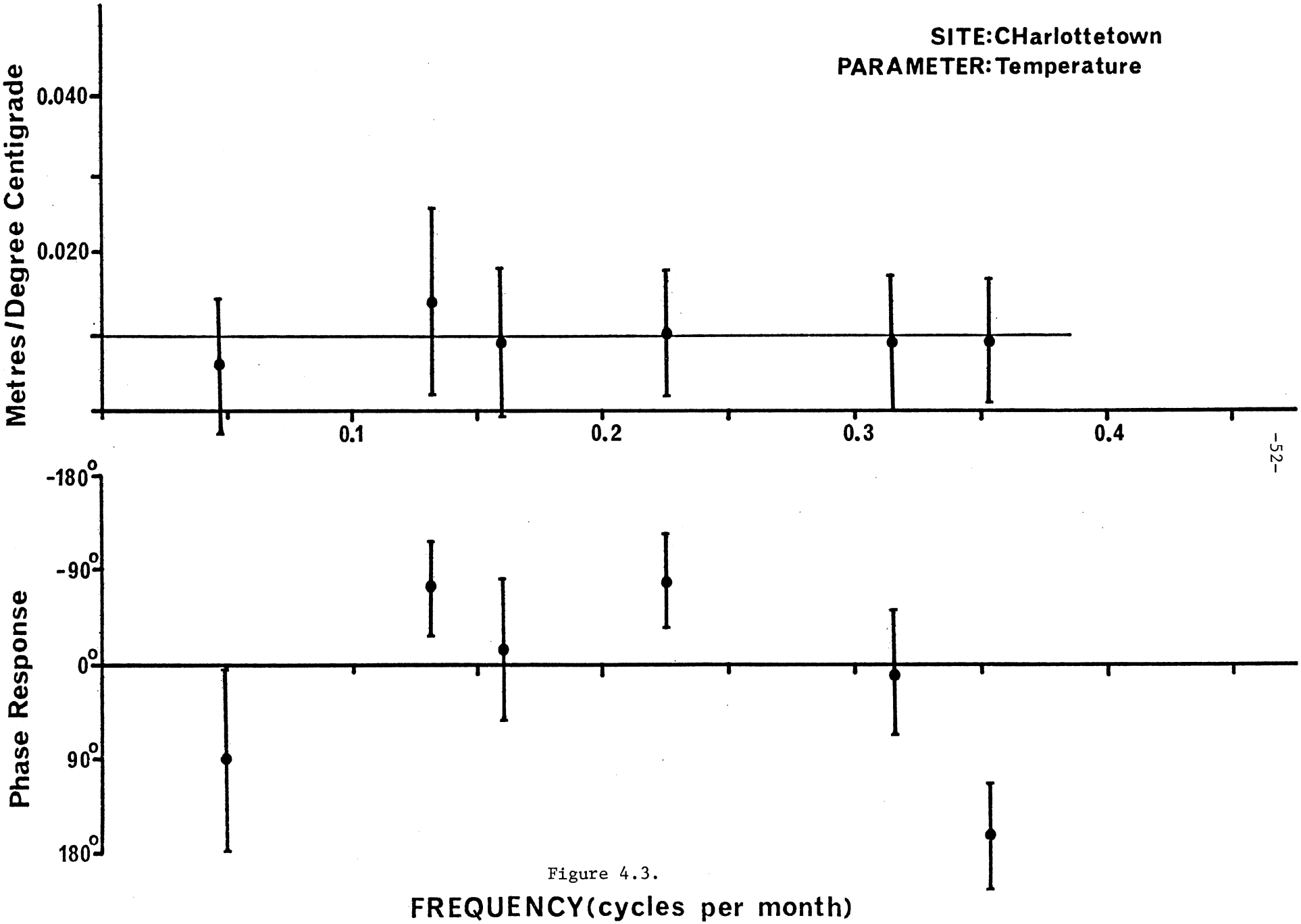
SITE:CHarlottetown
PARAMETER:Temperature
Metres/Degree Centigrade
0.040
0.020
0.1
0.2
0.3
0.4
Phase Response
-180°
-90°
0°
90°
180°
FREQUENCY(cycles per month)

Figure 4.3.

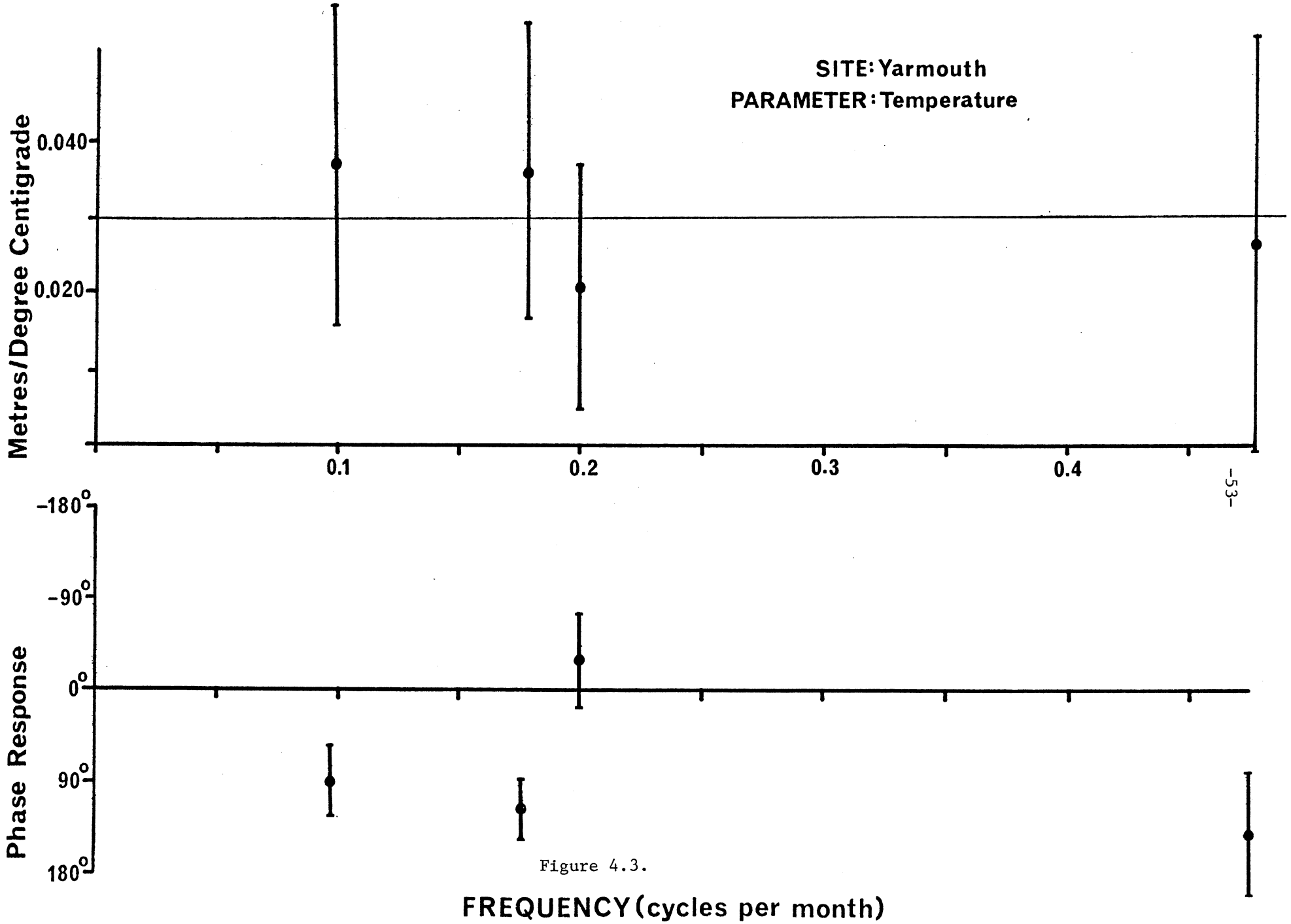
SITE: Yarmouth
PARAMETER: Temperature
Metres/Degree Centigrade
0.040
0.020
0.1
0.2
0.3
0.4
Phase Response
-180°
-90°
0°
90°
180°
FREQUENCY (cycles per month)

Figure 4.3.

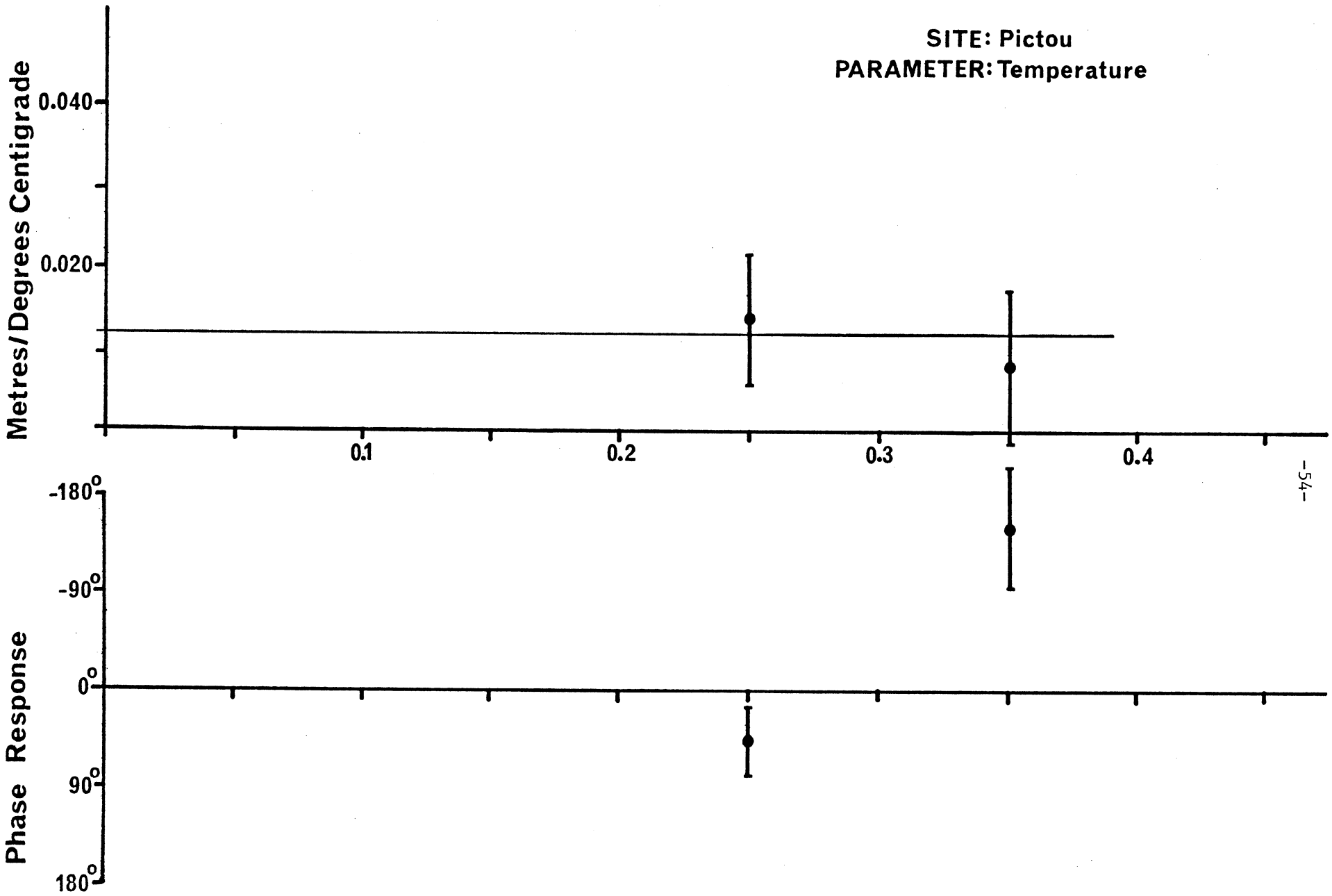
SITE: Pictou
PARAMETER: Temperature
Metres/Degrees Centigrade
0.040
0.020
0.1
0.2
0.3
0.4
-180°
-90°
0°
90°
180°
Phase Response
FREQUENCY (cycles per month)

Figure 4.3.

in any of the observed sea level records. A number of possible explanations for this discrepancy exist. Firstly, the temperature amplitude response may have been over-estimated (by a factor near two?), due to interference from an unmodelled influence of salinity or current variations. Secondly, the temperature amplitude response may be real, but its influence at the annual period may be diminished by that of another parameter, 180° out of phase with it. A possible candidate is the gravitational attraction of the sun, which reaches its maximum (solar perigee) near the time of minimum temperature in the Northern hemisphere. However, the theoretical amplitude of this tidal constituent is less than 10 mm (Lisitzin, 1974), and there appears to be no evidence for the ten-fold amplification needed here. Further investigation of this problem is certainly needed.

4.2.3 River Discharge

River discharge data were available for three ports. Of these, the small volume discharge, coupled with the short data span at Pictou, prevented any meaningful result being determined at this site. The frequency responses at the two remaining sites, Saint John and Father's Point, are shown in figure 4.4.

At Saint John, there appears to be a steady decrease in the amplitude factor with increasing frequency, and the phase response is near zero, as anticipated. At Father's Point the amplitude response is smaller, and does not appear to be frequency dependent. The magnitude of the amplitude response at Father's Point (20 mm per $10^{-3}m^3s^{-1}$) is similar to that which can be inferred from the results of Meade and

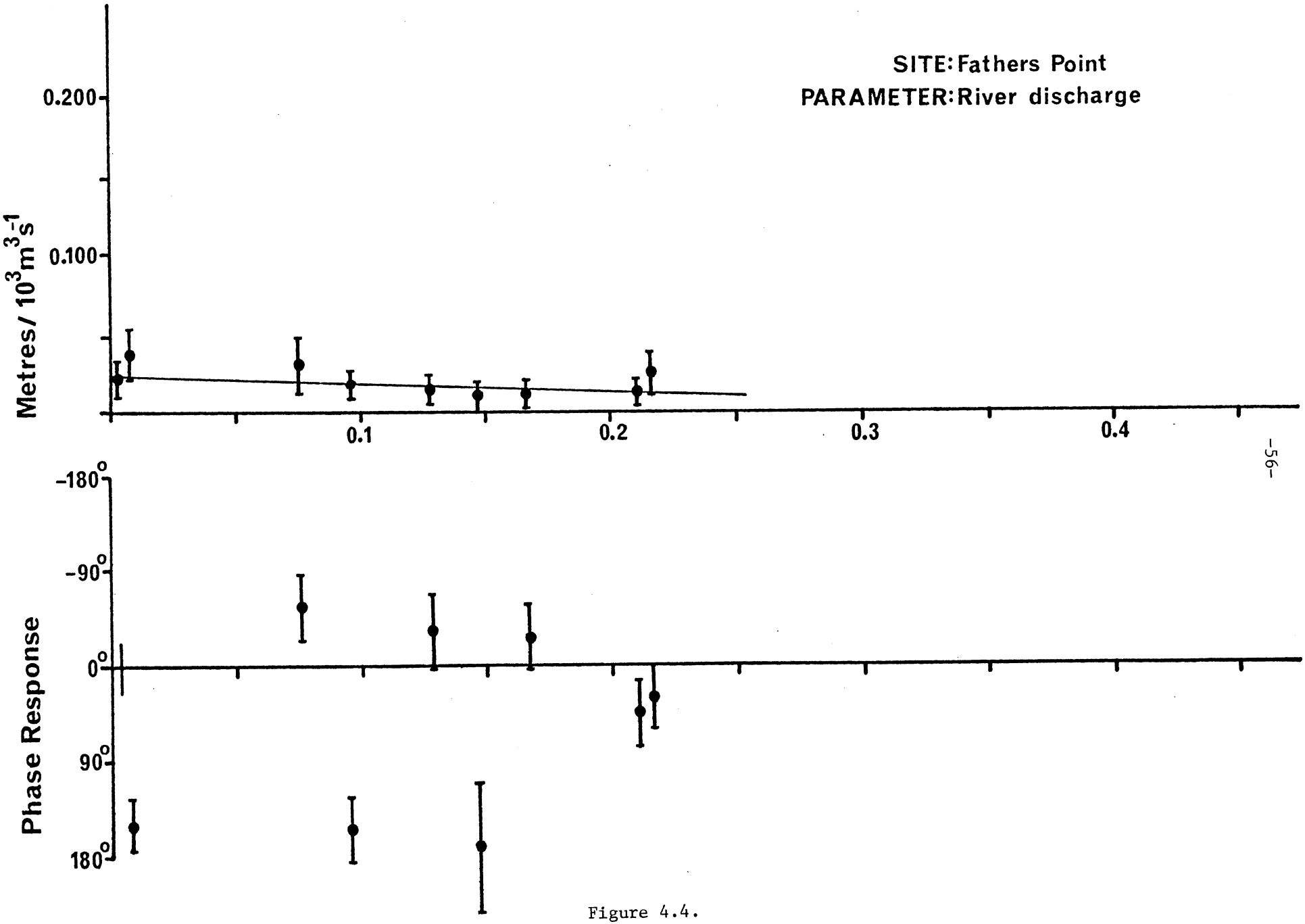
SITE: Fathers Point
PARAMETER: River discharge
0.200
0.100
Metres/ $10^3 m^3 s^{-1}$
0.1
0.2
0.3
0.4
-180°
-90°
0°
90°
180°
Phase Response
FREQUENCY(cycles per month)

Figure 4.4.

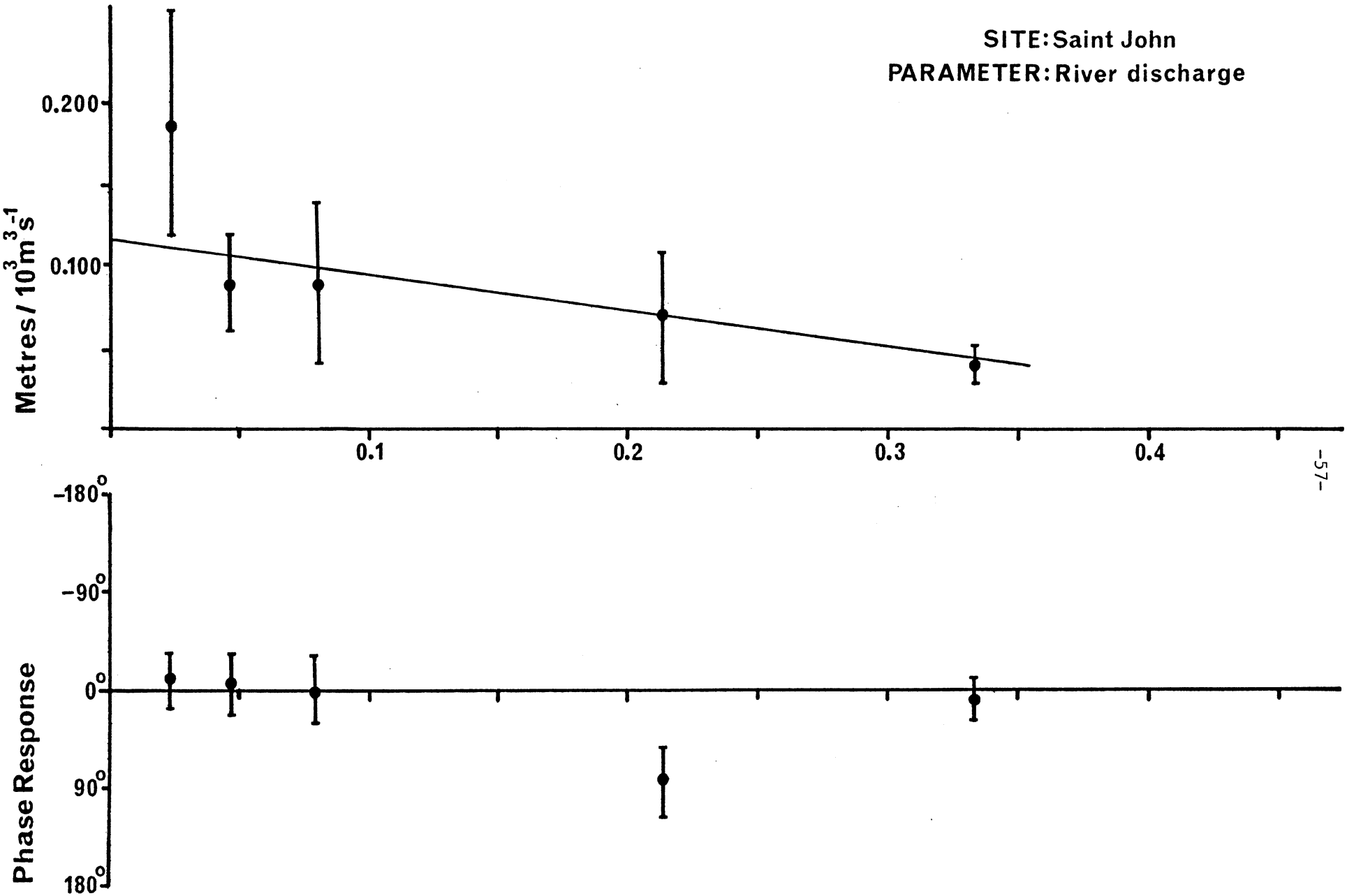
SITE: Saint John
PARAMETER: River discharge
0.200
0.100
Metres / 10^3 m^3 s^{-1}
0.1
0.2
0.3
0.4
-180°
-90°
0°
90°
180°
Phase Response
FREQUENCY (cycles per month)

Figure 4.4.

Emery (1971). For Father's Point, the phase response at most frequencies is near zero, as anticipated. However, at three frequencies, this response is near 180°. This phase switch is at present inexplicable, and warrants further investigation.

4.2.4 Wind Stress

The determination of the wind stress response has caused further problems. For the purpose of determining the stress components normal and tangential to the coastline, the average trend of the coastline over a one hundred kilometre length was used to define its orientation. Based upon elementary principles, the anticipated effect of a wind blowing towards the shore would be a piling up of the water at the coastline, resulting in a rise in sea level (Lisitzin, 1974). Using similarly basic principles, the effect of a tangential (longshore) wind would result in an average water movement to the right (in the Northern hemisphere). This effect is known as Ekman transport (Knauss, 1978). For a shoreline to the right of the wind, this would again result in a rise in sea level. With the coordinate conventions adopted in chapter 3, the expected phase response for both normal and longshore wind stress components is 0°. However, in most cases, the phase response was poorly determined, and in some cases tended towards 180°.

In an attempt to improve the determination of this phase factor, the wind stress at all sites was recomputed, using the local (within a few kilomitres) orientation of the shoreline. It is these results which are displayed in figure 4.5. The consistency (at any one site) of the phase response has been improved, but most phase factors are

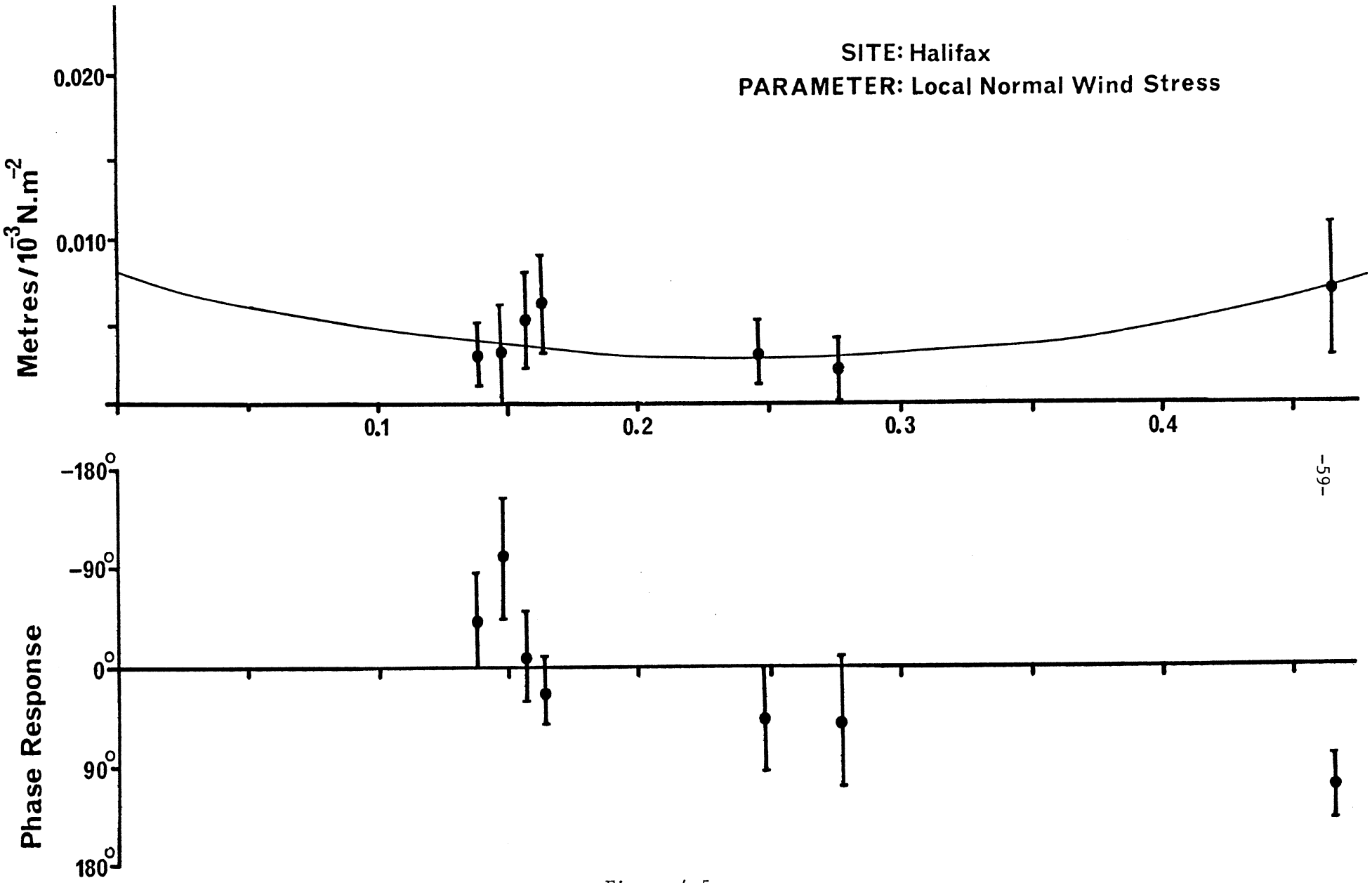
SITE: Halifax
PARAMETER: Local Normal Wind Stress
Metres/10^-3 N.m^-2
0.020
0.010
0.1
0.2
0.3
0.4
Phase Response
-180°
-90°
0°
90°
180°
FREQUENCY (cycles per month)

Figure 4.5.

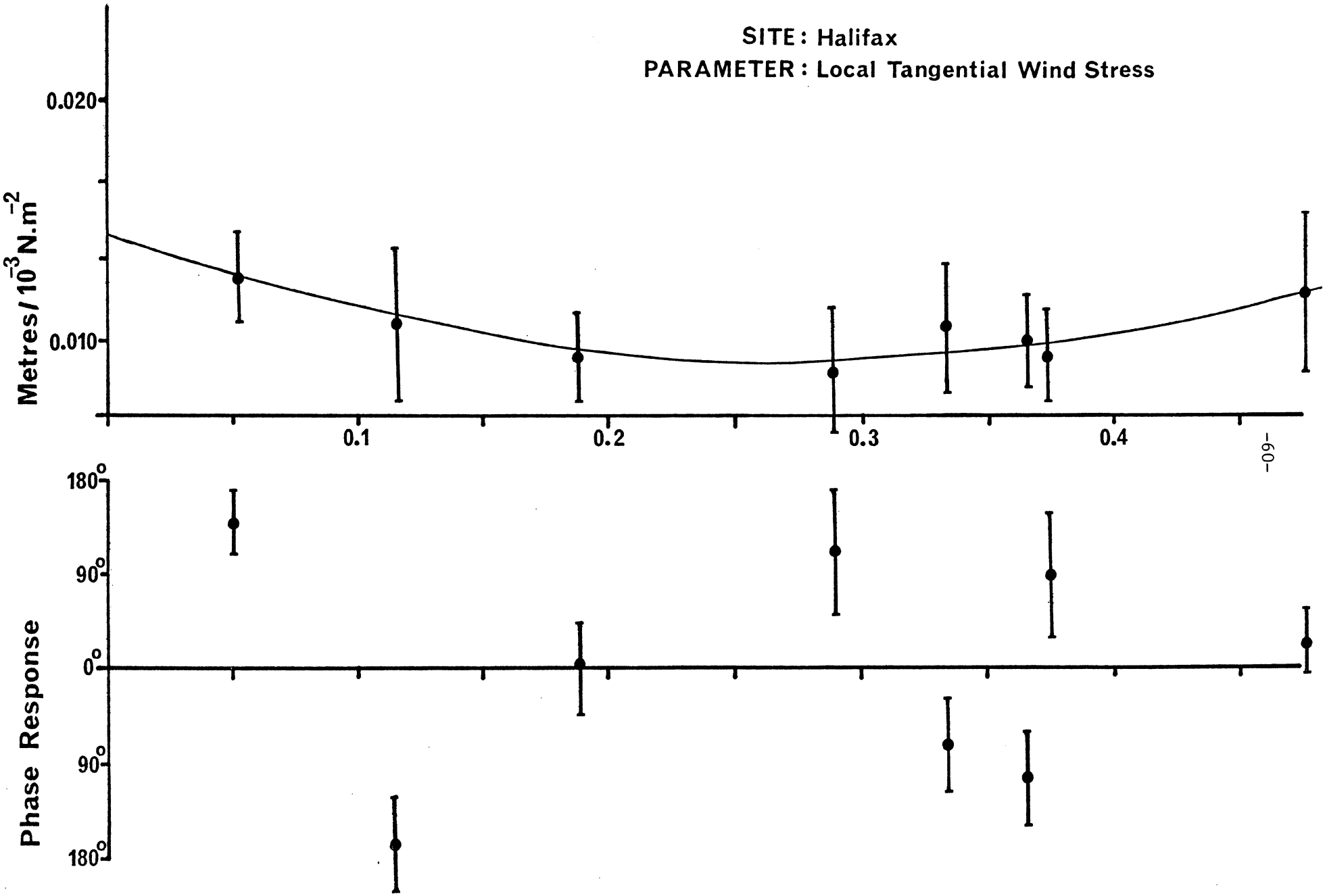
SITE : Halifax
PARAMETER : Local Tangential Wind Stress
0.020
0.010
Metres/ 10^{-3} N.m^{-2}
0.1
0.2
0.3
0.4
180°
90°
0°
90°
180°
Phase Response
FREQUENCY(cycles per month)

Figure 4.5.

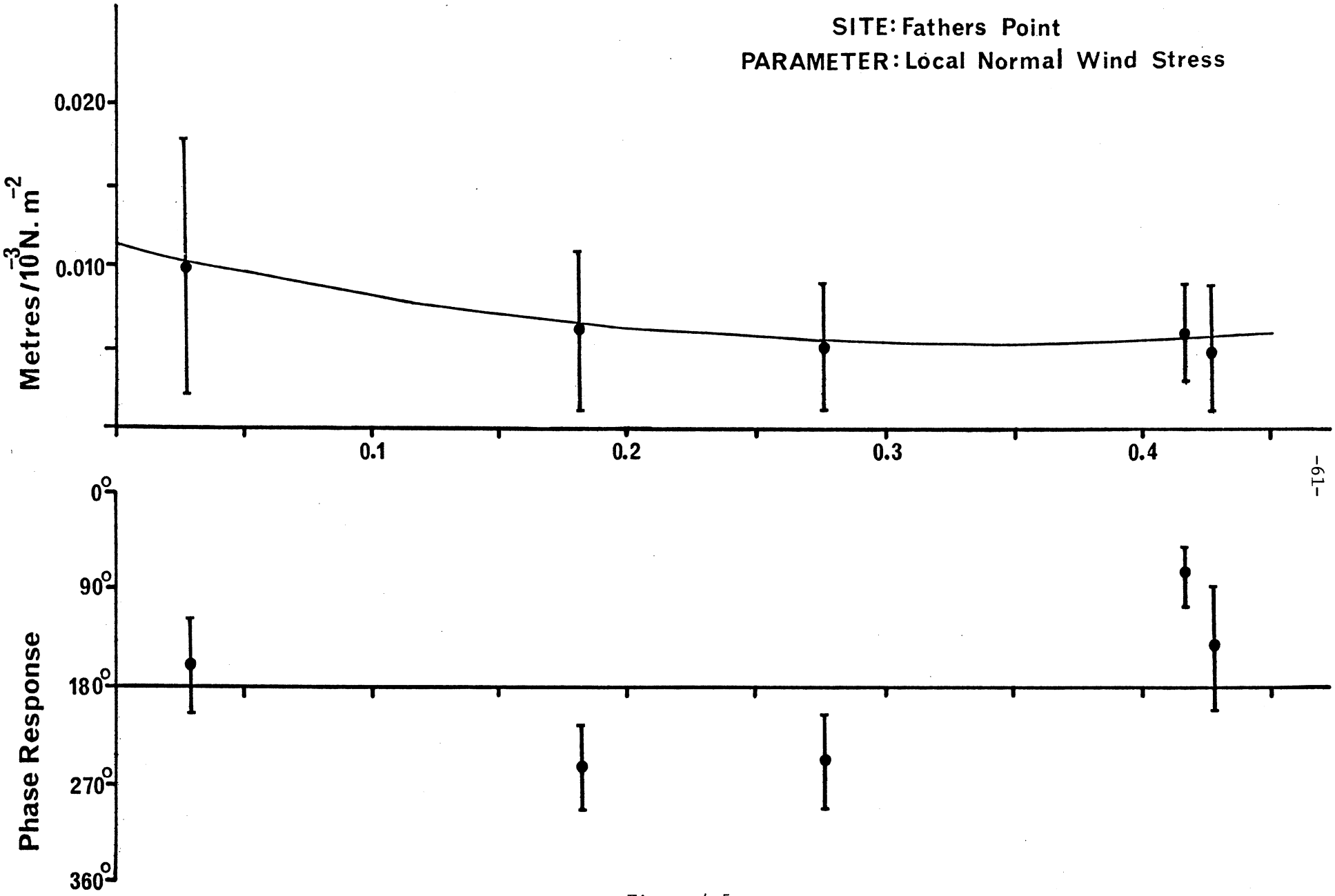
SITE: Fathers Point
PARAMETER: Local Normal Wind Stress
0.020
0.010
Metres/10^-3 N. m^-2
0.1
0.2
0.3
0.4
0°
90°
180°
270°
360°
Phase Response
FREQUENCY (cycles per month)

Figure 4.5.

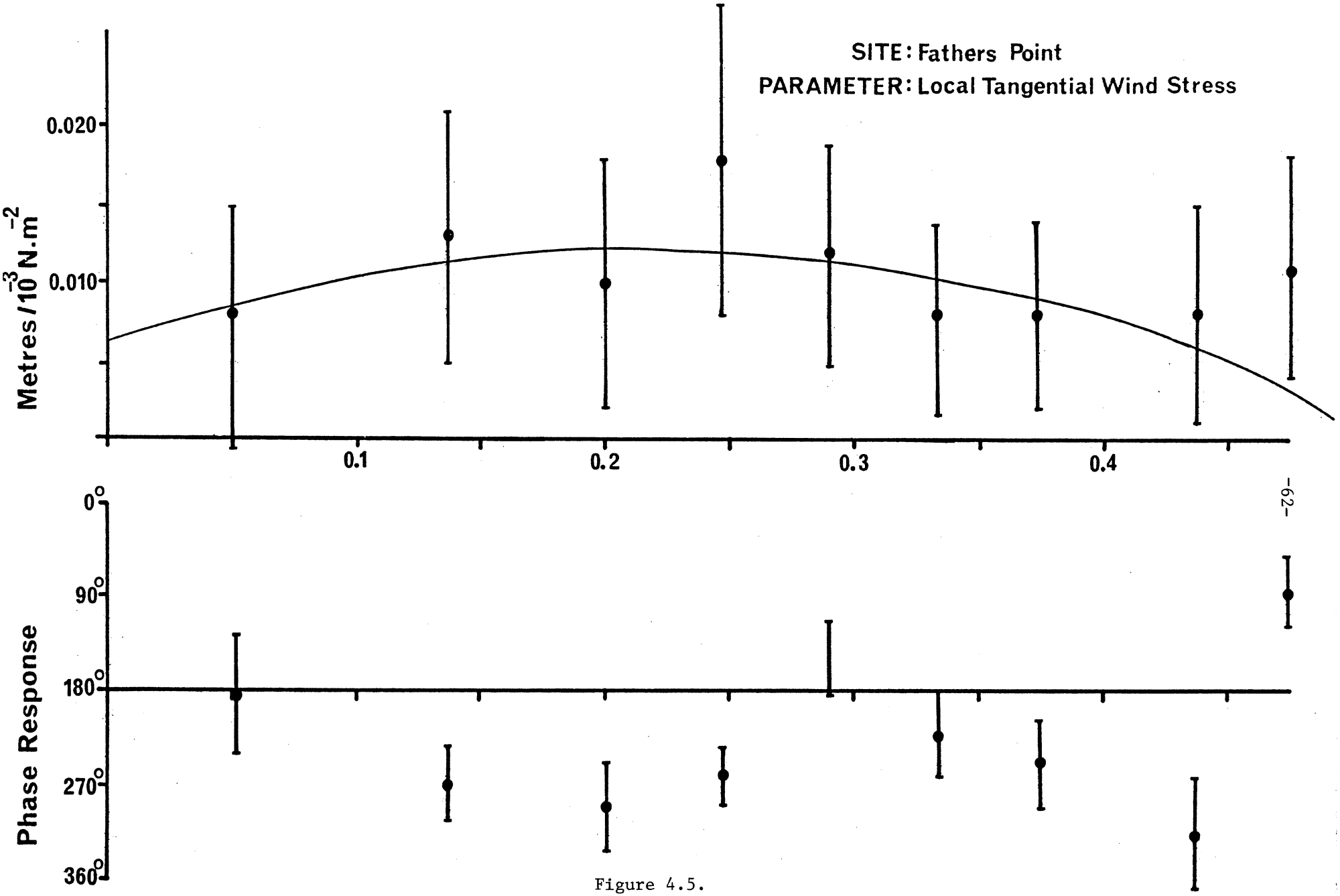
SITE: Fathers Point
PARAMETER: Local Tangential Wind Stress
Metres/10^-3 N.m^-2
0.020
0.010
0.1
0.2
0.3
0.4
Phase Response
0°
90°
180°
270°
360°
FREQUENCY (cycles per month)

Figure 4.5.

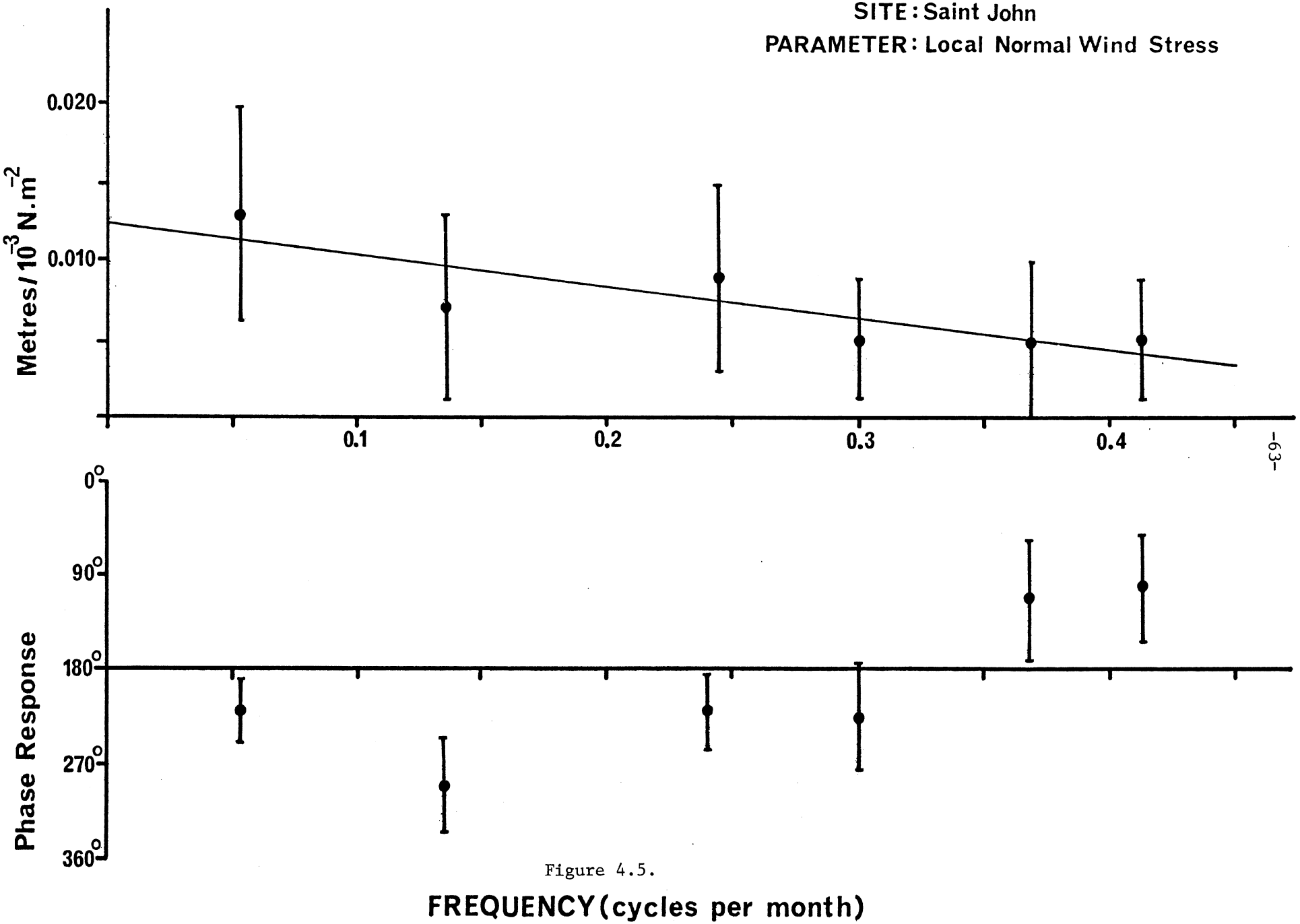
SITE: Saint John
PARAMETER: Local Normal Wind Stress
0.020
0.010
Metres/10^{-3} N.m^{-2}
0.1
0.2
0.3
0.4
0°
90°
180°
270°
360°
Phase Response
FREQUENCY (cycles per month)

Figure 4.5.

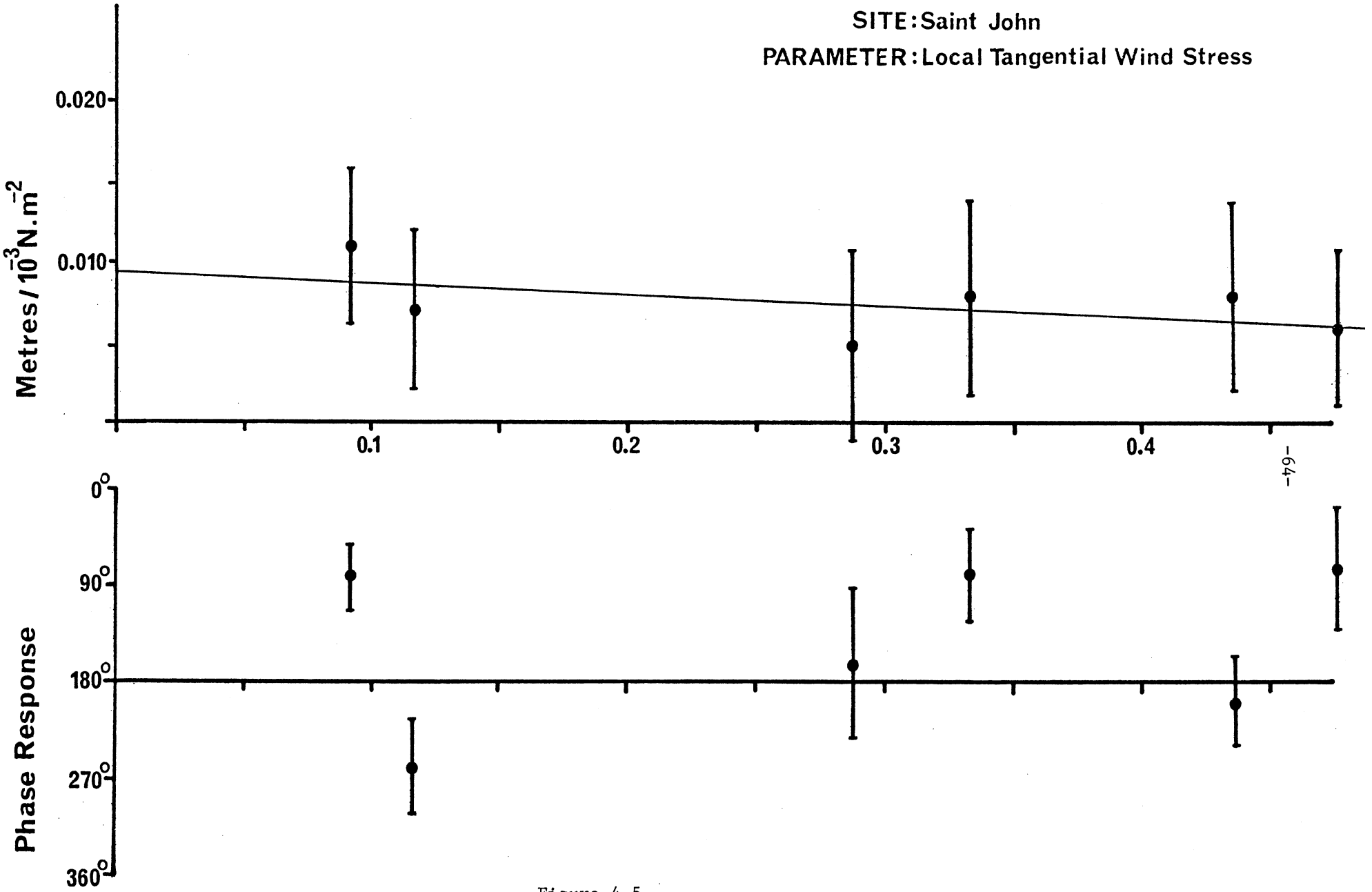
SITE: Saint John
PARAMETER: Local Tangential Wind Stress
0.020
0.010
Metres / 10^{-3} N.m^{-2}
0.1
0.2
0.3
0.4
0°
90°
180°
270°
360°
Phase Response
FREQUENCY (cycles per month)

Figure 4.5.

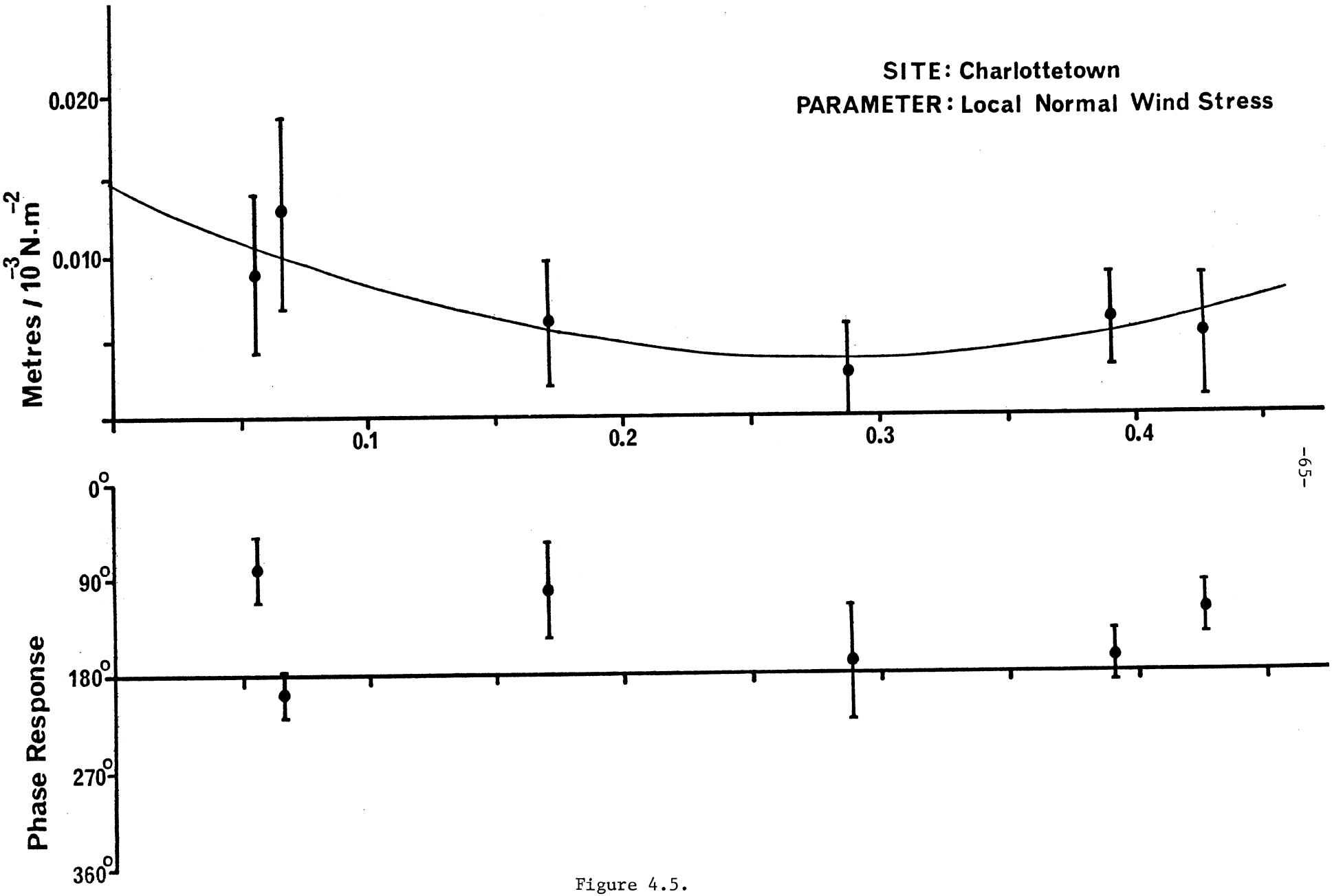
SITE: Charlottetown
PARAMETER: Local Normal Wind Stress
Metres / 10^{-3} N.m^{-2}
0.020
0.010
0.1
0.2
0.3
0.4
Phase Response
0°
90°
180°
270°
360°
FREQUENCY (cycles per month)

Figure 4.5.

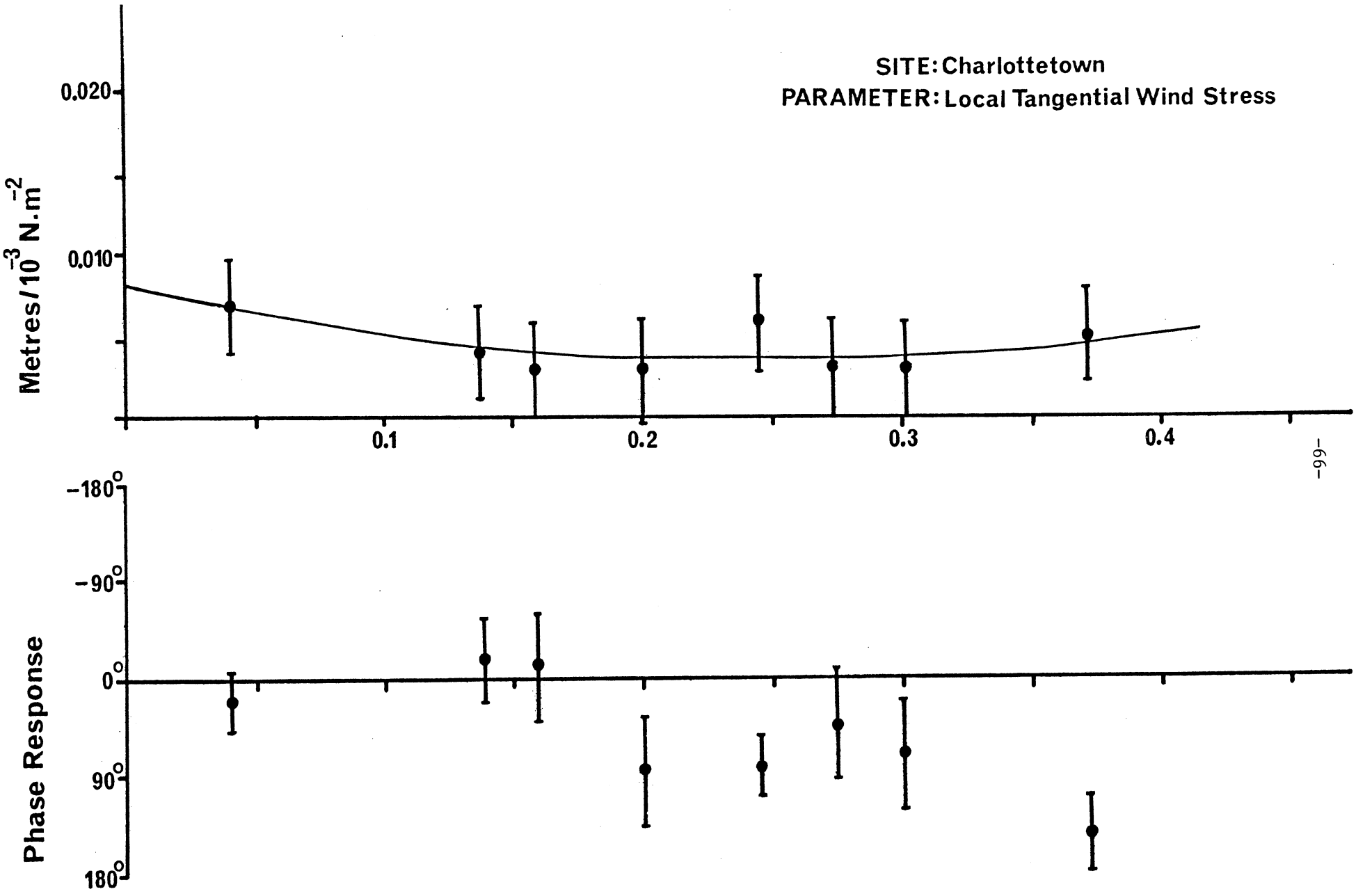
SITE: Charlottetown
PARAMETER: Local Tangential Wind Stress
0.020
0.010
Metres/10^-3 N.m^-2
0.1
0.2
0.3
0.4
-180°
-90°
0°
90°
180°
Phase Response
FREQUENCY (cycles per month)

Figure 4.5.

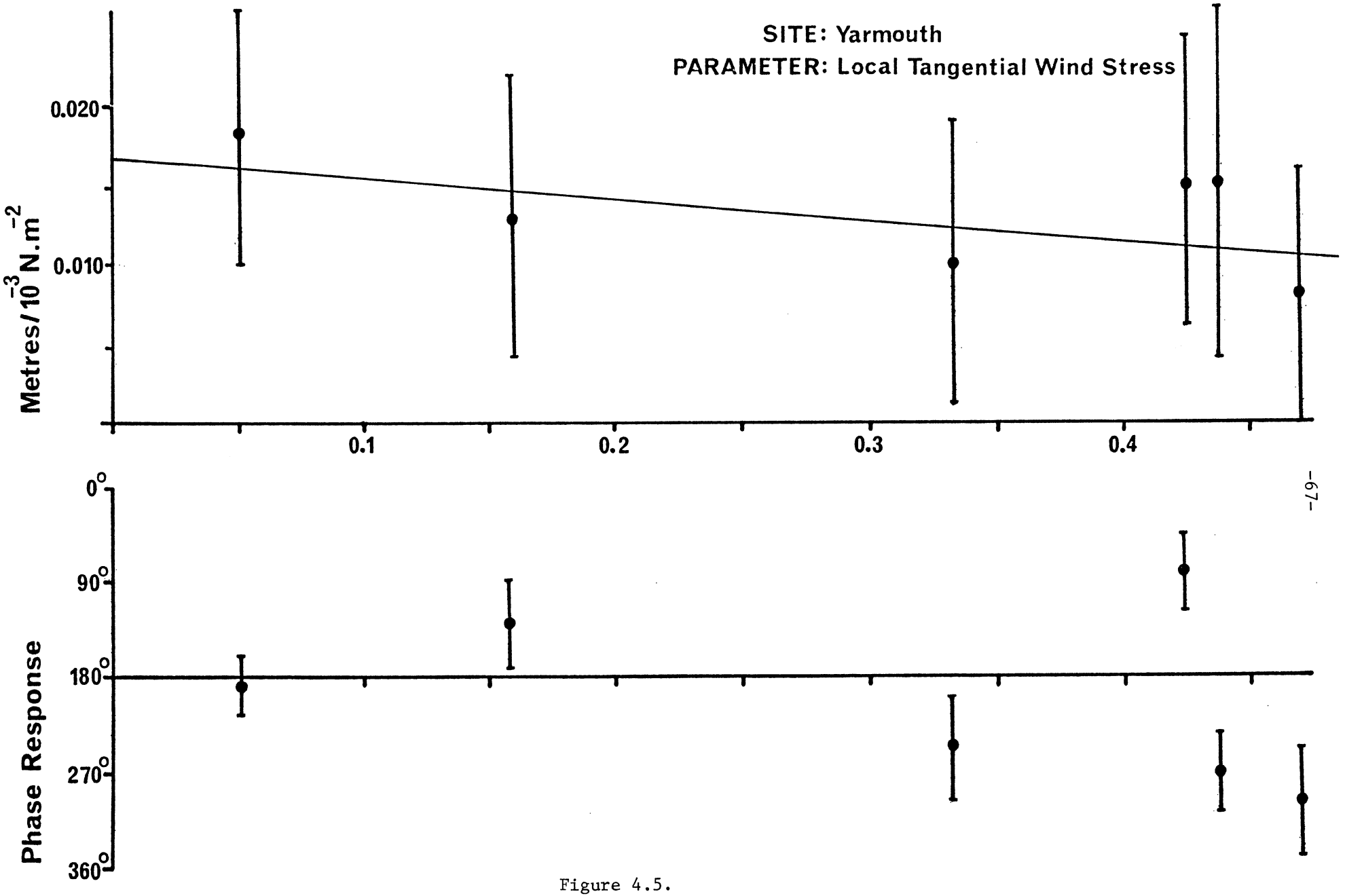
SITE: Yarmouth
PARAMETER: Local Tangential Wind Stress
0.020
0.010
Metres/10^-3 N.m^-2
0.1
0.2
0.3
0.4
0°
90°
180°
270°
360°
Phase Response
FREQUENCY(cycles per month)

Figure 4.5.

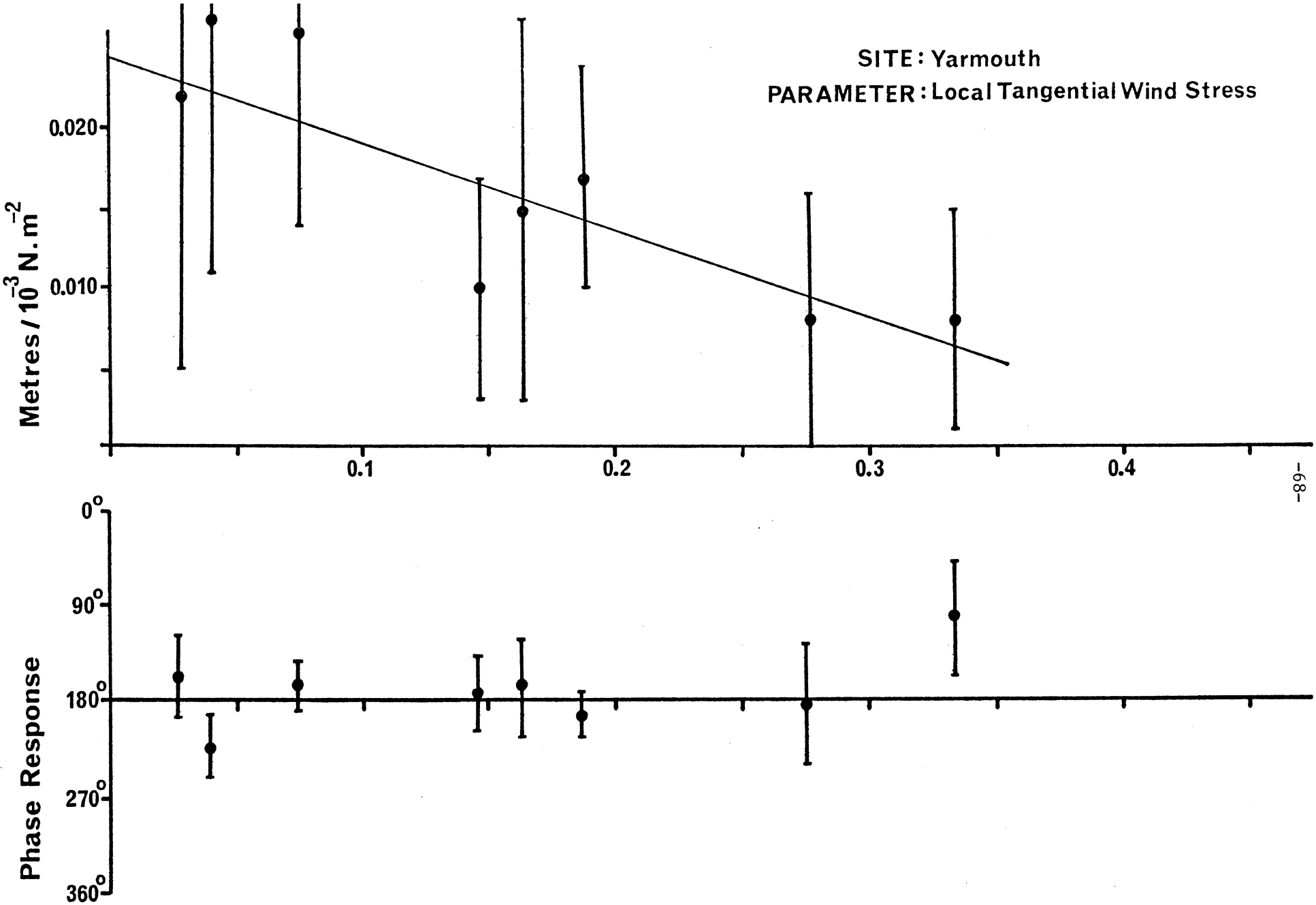
SITE : Yarmouth
PARAMETER : Local Tangential Wind Stress
Metres / 10^{-3} N.m^{-2}
0.020
0.010
0.1
0.2
0.3
0.4
Phase Response
0°
90°
180°
270°
360°
FREQUENCY(cycles per month)

Figure 4.5.

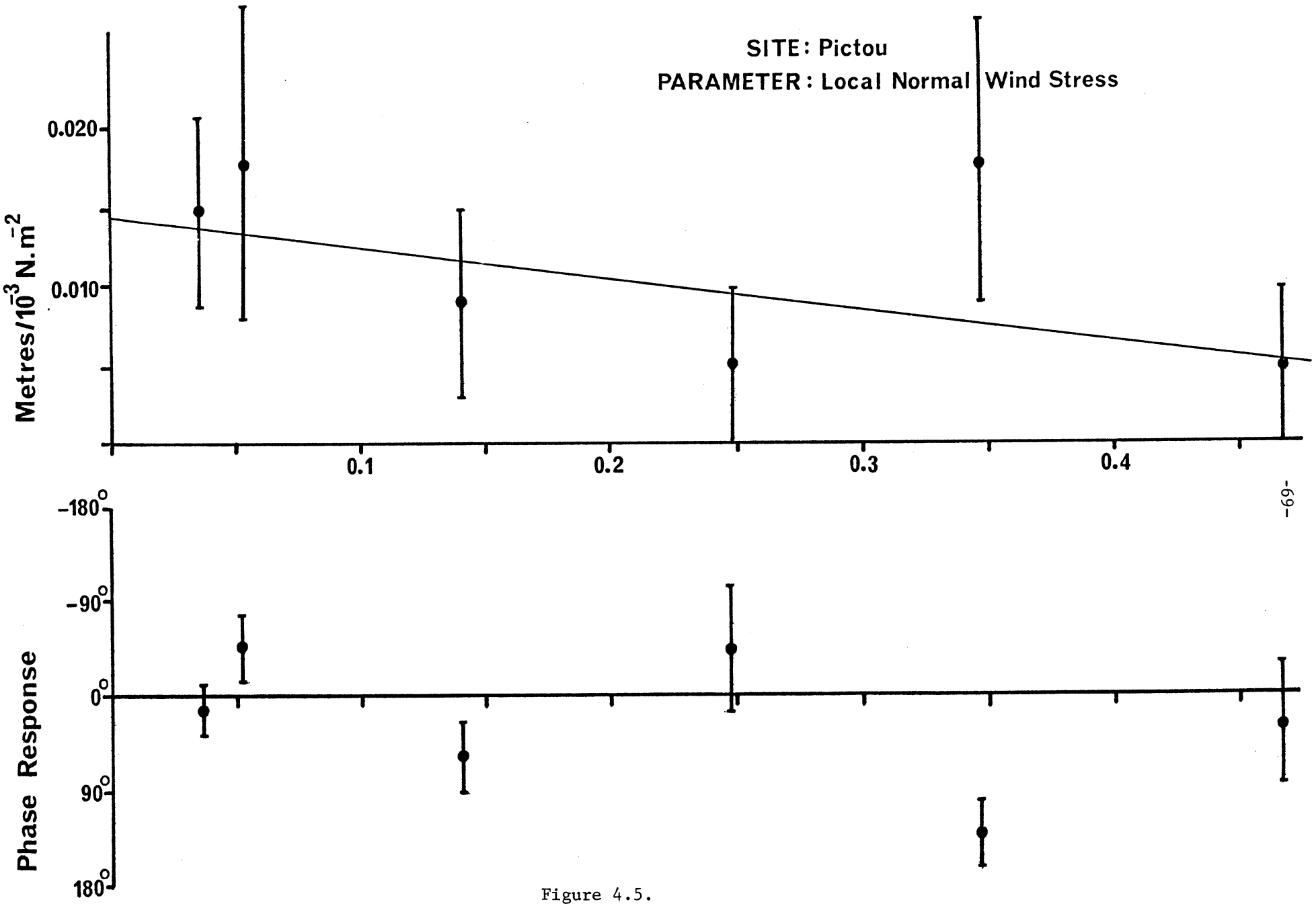
SITE: Pictou
PARAMETER: Local Normal Wind Stress
Metres/10^-3 N.m^-2
0.020
0.010
0.1
0.2
0.3
0.4
Phase Response
-180°
-90°
0°
90°
180°
FREQUENCY (cycles per month)

Figure 4.5.

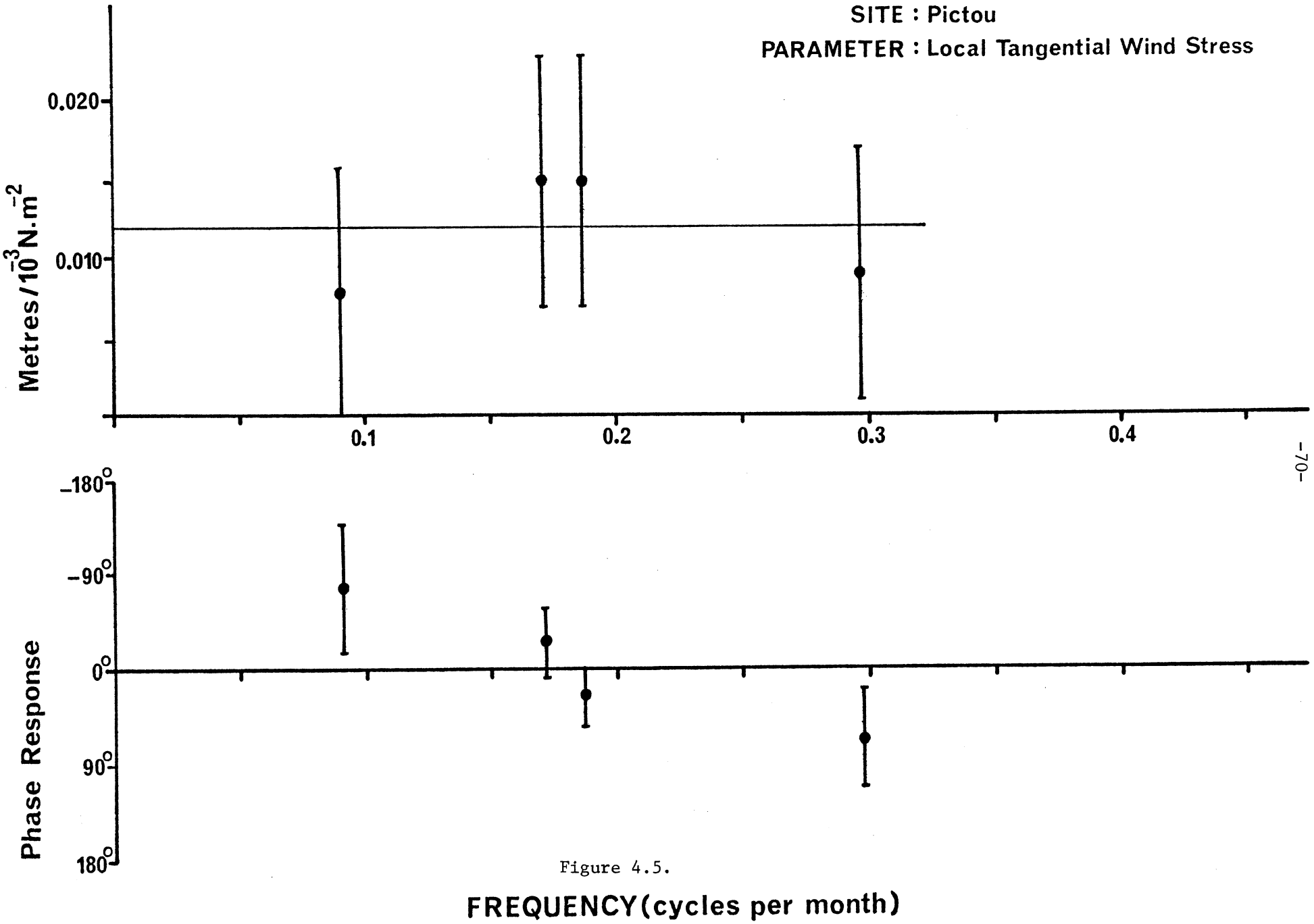
SITE : Pictou
PARAMETER : Local Tangential Wind Stress
0.020
0.010
Metres/10^{-3}N.m^{-2}
0.1
0.2
0.3
0.4
-180°
-90°
0°
90°
180°
Phase Response
FREQUENCY(cycles per month)

Figure 4.5.

still near 180°. The responses of both normal and tangential components are of a similar magnitude, which result agrees with that of Noble and Butman (1979) for the Gulf of Maine, but contrasts with the results of Wong (1975), who found that the longshore wind stress response is predominant. The average magnitude of the amplitude response determined in this study (8 mm per 10^{-3}N.m^{-2}) is 2-3 times larger than the values obtained by the above-mentioned investigators. The explanation for this discrepancy and for the 180° phase shifts at some sites, probably lies in a more careful analysis of the influences of local festures, both on wind velocity, and on wind-induced water transport. That the local topography can influence the response of sea level to wind forcing, even to the extent of an offshore wind inducing a rise in sea level, is well-documented in Miller (1958).

4.3 Zero Frequency Response

Of primary interest in this study is the response of sea level to meteorological forcing at zero frequency, adding to the quasi-stationary sea surface topography. This response can be determined by extrapolating the amplitude responses shown in figures 4.2 to 4.5 to zero frequency. This extrapolation can only be carried out reliably if the amplitude responses vary smoothly with frequency, exhibiting no resonant features. This appears to be the case with the results obtained here, and this confirms the "credo of smoothness" enforced by Munk and Cartwright (1966).

The fitting of the smooth curve to the amplitude response has been carried out using a least squares fit of a low-order algebraic polynomial. Denoting the amplitude response, $|H(f_j)|$, by the simpler

symbol, r_j, we have:

$$\hat{r}_j = \sum_{i=0}^{n}{}' a_j f_j^i \qquad j = 1,\ldots, m \quad , \tag{4.1}$$

where f_j is the frequency and the a_j are found from the weighted least squares solution:

$$\sum_{i=0}^{n} \langle f^k , f^i \rangle \cdot a_i = \langle f^k, r \rangle \qquad k = 1,\ldots,n \quad , \tag{4.2}$$

Here, the weights, ρ_j, are derived from the inverse squares of the standard errors, σ_j, associated with each r_j:

$$\rho_j = \sigma_j^{-2} \quad . \tag{4.3}$$

In the selection of a suitable order of polynomial, n, for each response function, the following two guidelines were used:

(i) n was kept at or below 3, so that the response function remained smooth.

(ii) For each response function, equation (4.2) was evaluated for n ranging from 0 to 3, and that value of n was chosen which provided the smallest variance. For a large sample size, the variance would steadily decrease with increasing n. However, for the small samples of frequencies available here, the significant reduction in the degrees of freedom incurred when using a higher value of n, can lead to a lower value producing a smaller variance.

The finally selected response functions have been drawn on figures 4.2 to 4.5, and the resulting zero frequency amplitude factors, together with their associated standard errors, are listed in table 4.2.

4.4. Relative Sea Surface Topography

In order to determine the sea surface topography it is necessary to know the local anomalies of the forcing parameters which would cause a separation of mean sea level from the geoid. In the cases of wind stress and river discharge this is comparatively easy - any

SITE	PRESSURE mm/mbar	TEMPERATURE mm/°C	RIVER DISCHARGE $mm/10^{3} \cdot m^{3}s^{-1}$	WIND STRESS $mm/10^{-3}N \cdot m^{-2}$	
				NORMAL	TANGENTIAL
Halifax	11 ± 2	21 ± 3	-	8 ± 4	11 ± 1
Father's Pt.	14 ± 2	23 ± 10	22 ± 5	11 ± 2	6 ± 4
St. John	9 ± 1	18 ± 4	114 ± 21	12 ± 2	9 ± 2
Chartotte-town	12 ± 2	9 ± 1	-	14 ± 3	8 ± 1
Yarmouth	15 ± 4	30 ± 4	-	17 ± 3	24 ± 4
Pictou	15 ± 2	12 ± 3	-	14 ± 4	12 ± 2

Table 4.2: Zero Frequency Amplitude Responses

value different from zero will force a departure of sea level from the geoid. It is sufficient to calculate the average values of wind stress and river discharge at each site, and to multiply these values by the appropriate zero frequency amplitude responses, in order to determine their contribution to the sea surface topography.

In the cases of the atmospheric pressure and air temperature, it is clear, from the difinition of the geoid, that differences from a global mean pressure and air temperature are needed at each site. It is also clear that these "global means" should only be taken over the oceans. A value for the global average pressure over the oceans of 1011,06 mbar has been determined (Lisitzin, 1974). However, no corresponding value for air temperature could be found, and we must content ourselves with using a regional mean value. We will not then be able to determine the absolute sea surface topography, but only the relative topography (and then only for the influences described here - no account has been taken of salinity and current effects). The approach adopted here has been to take the (time) averages of air temperature at each site, and then to compute a regional mean value from these averages. The departures form this regional mean at each site can then be used to calculate the regional relative sea surface topography. For atmospheric pressure, departure from the global mean are calculated. These departures, and the mean wind stress and river discharge values, together with their precision estimates, are summarized in table 4.3.

The results listed in tables 4.2 and 4.3 may be combined to provide estimates of the contribution to the quasi-stationary sea surface topography from each influence. These estimates are summarized

SITE	PRESSURE MILLIBARS MEANS	DEPARTURE	TEMPERATURE °C MEAN	DEPARTURE	RIVER DISCHARGE 10^3 $m^3 s^{-1}$	WIND STRESS $10^{-3} N \cdot m^{-2}$ NORMAL	TANGENTIAL
Halifax	1013,93	± 2,87	7,51	+1.76	-	-4,313	+2,915
	± 0,19		±0,07			±0,280	±0,186
Father's Pt.	1013,38	+ 2.32	2,68	-3.07	11,188	+2,655	+2,916
	± 0,14		±0.09		± 0.137	±0,376	±0.174
St.John	1010,08	+3,02	5,82	+0,07	0,742	+3,137	-0,916
	± 0,17		±0,07		± 0,033	±0,191	±0,195
Charlotte-town	1013,41	+2,35	5,48	-0,27	-	-2,693	-5,073
	± 0,16		±0,09			±0,243	±0,271
Yarmouth	1014,94	+3,88	6,76	+1,01	-	+3,050	+1,226
	± 0,16		±0,10			±0,192	±0.227
Pictou	1013,93	+2,87	6,27	+0,52	-	-6,011	-0,822
	± 0,22					±0,286	±0,243
Mean	1011,06 (Global)	-	5,75 Regional)	-	-		

Table 4.3: Mean Values of Meteorological Influences

in table 4.4. Some comments on these results are appropriate.

The influence of atmospheric pressure is to force a depression in the sea surface over the entire region of about 30 mm, with respect to the global sea level. This depression is consistent with Lisitzin's (1974) chart. Within the region, there is some variations, with the sites containing the shorter data spans (Yarmouth and Pictou) exhibiting the largest depression of sea level. This probably reflects a weaker determination of the pressure amplitude response, rather than any acutal deviation from the regional average.

The temperature effect fluctuates significantly within the region, with the largest effect (in magnitude) being at Father's Point. As mentioned earlier, these results should be treated with caution, as it is unclear, as yet, whether the temperature amplitude response has been overestimated or not. It is probable that the regional mean air temperature of 5,75°C is lower than the global average over the oceans, but it has not been possible to obtain such a figure.

The large river discharge effect at Father's Point is the most noticeable feature of these results, and does appear to be real. The amplitude response is well-determined (figure 4.4), and its magnitude is in good agreement with that implied in Meade and Emery (1971). Using a different approach, Anderson (1978), obtained an amplitude response at Father's Point approximately one-third the size of that obtained here. However, a direct comparison of these results may be misleading, as the earlier investigations did not take into account contributions from other sources.

With regard to the wind stress contribution, the results shown

SITE	PRESSURE	TEMPERATURE	RIVER DISCHARGE	WIND STRESS NORMAL	WIND STRESS TANGENTIAL	TOTAL MILLIMETRES
Halifax	-32 ± 6	+37 ± 5	-	-34 ± 17	+32 ± 4	+3 ± 19
Father's Point	-32 ± 5	-71 ± 31	+246 ± 56	-29 ± 7	-17 ± 12	+97 ± 66
St. John	-27 ± 3	+1 ± 1	+ 85 ± 16	-38 ± 7	+ 8 ± 3	+29 ± 18
Charlotte-town	-28 ± 5	-2 ± 1	-	+38 ± 9	-41 ± 6	-33 ± 12
Yarmouth	-58 ± 16	+30 ± 5	-	-52 ± 10	-29 ± 7	-109 ± 21
Pictou	-43 ± 7	+ 6 ± 2	-	-84 ± 24	-10 ± 3	-131 ± 25

Table 4.4: Relative Local Variations of Sea Surface Topography.

take into account the phase responses indicated in figure 4.5. At some of the sites, the effects of the two components tend to cancel, while at others (Father's Point, Yarmouth, Pictou) they do not. At Father's Point and Yarmouth a depression of sea level has resulted from a wind that, on average, blows from water to land. This result contradicts the expected piling up effect, but may be partially explained in terms of the local situation. At Father's Point, the tide gauge is sheltered from a North-westerly induced pile up by a quay. At Yarmouth, a similar situation occurs with the Westerly winds. At Pictou, the average wind blows from the land to the sea, and the expected depression of sea level occurs.

The total contribution towards the sea surface topography ranges from near zero at Halifax to 13 cm at Pictou. These contributions are significant (at the 95% confidence level) at Charlottetown, Yarmouth, and Pictou only. However, the error estimates used in determining the significance levels should be treated with some reserve. These estimates are based upon the precision estimates for the zero frequency amplitude factors (table 4.2), which are no more than estimates of the goodness of fit of the low-order polynomial to the data. It is likely that the error estimates for the contribution towards sea surface topography at the sites with short mean sea level records (Yarmouth and Pictou) are considerably over-optimistic.

In the absence of an estimate for a global average air temperature over the oceans, the total contributions listed in table 4.4 can only be used in a relative sense. Even then, influences such as salinity and currents may considerably modify the differences in sea surface topography between pairs of ports.

Of direct practical interest is whether these differences in sea surface topography would significantly distort the precise level network linked to the tide gauges. Or, approaching the problem from a different aspect, could these precise level connections be used to detect differences in sea surface topography? This problem will be more fully investigated at a later date.

5. Conclusions

The purpose of the investigation described in this report was to determine the permanent response of the sea level to phenomena such as atmospheric pressure, temperature, wind and river discharge. The overall response can be sought in two components - as an amplitude factor and a phase lag - both as functions of frequency. The standard approach to studying such a response is based on cross-spectra and has been used in the field of electrical engineering for a long time. The alternative "Response method", introduced into oceanography by Munk and Cartwright in 1966, has been used principally to study the behaviour of the sea in the high frequency domain - for diurnal and semidiurnal tides.

We have attempted to model the response in the low frequency domain (0.1 to 6 cycles per year) and extrapolated it to zero frequency. The zero-frequency (permanent) response can be used to estimate the quasi-stationary local contributions to sea surface topography, knowing the quasi-stationary departures (long-term local mean departures from global means) of the forcing parameters.

Three mathematical techniques were investigated for versatility in this context, where both the input and output series must be considered contaminated by noise; signal to noise ratio as low as 0.5 occurs. These techniques were: the cross-spectral analysis, Munk - Cartwright's weighting function technique and the response method designed by R.R. Steeves based on least-squares spectral analysis. It was found that the last technique performs the best in our circumstances.

Consequently, this technique has been used to evaluate the permanent response of the sea level in Halifax, Yarmouth, Saint John, Father's Point, Charlottetown and Pictou, all ports in eastern Canada. From the determined responses and from the semi-permanent atmospheric anomalies the relative local variations of sea surface topography were estimated, together with their standard deviations.

Neither water temperature nor salinity records were available at the investigated ports. Also, it was beyond our competence to evaluate the effect of ocean currents and the sea-bed shape; this evaluation, we feel, falls into the field of physical oceanography. The results obtained by us are thus incomplete in so far as they do not represent the entire sea surface topography. We think, however, that they do represent at least a significant part of the local variations.

The obtained results should be compared with results obtained from geodetic levelling between the pertinent pairs of ports. Another study called for, before any more definitive conclusions can be reached, is that of a sea-level response to regionally more coherent forcing parameters. It would be very interesting to establish if an enforced regional coherence would change the local sea level departures appreciably.

REFERENCES

Anderson, E.G. (1978). Modelling of Physical Influences in Sea Level Records for Vertical Crustal Movement Detection. Proc. of the 9th GEOP Conference, Columbus, Ohio.

Bendat, J.S. and A.G. Piersol (1971). Random Data: Analysis and Measurement Procedures. Wiley-Interscience, New York.

Cartwright, D.E. (1969). A Unified Analysis of Tides and Surges Round North and East Britain. Phil. Trans. Roy. Soc. London (Series A), 263, 1-55.

Castle, R.O. and P. Vanicek (1980). Interdisciplinary Considerations in the Formulation of the New North American Vertical Datum, Proc. NAD Symposium 1980 (Ed. G. Lachapelle), Ottawa, May, pp. 285-299.

Delikaraoglou, D. (1980). Sea Surface Computations from Local Satellite Tracking and Satellite Altimetry. University of New Brunswick, Dept. of Surveying Engineering, Technical Report 74.

Godin, G. (1972). The Analysis of Tides. University of Toronto Press, Toronto.

Hamon, B.V. (1966). Continental Shelf Waves and the Effects of Atmospheric Pressure and Wind Stress on Sea Level. J. of Geophysical Research 71(12), pp. 2883-2893.

Knauss, J.A. (1978). Introduction to Physical Oceanography. Prentice-Hall, New Jersey.

Lisitzin, E. (1974). Sea Level Changes. Elsevier, Amsterdam.

Mather, R.S. (1974). Quasi-Stationary Sea Surface Topography and Variations of Mean Sea Level with Time. Unisurv. G. 21, pp. 18-73.

Meade, R.H. and K.O. Emery (1971). Sea Level as Affected by River Runoff, Eastern United States. Science, 173, pp. 425-428.

Miller, A.R. (1958). The Effects of Winds on Water Levels on the New England Coast. Limnology and Oceanography, 3(1): 1-14.

Munk, W.J. and D.E. Cartwright (1966). Tidal Spectroscopy and Prediction. Phil. Trans. Roy. Soc. London (series A), 259, pp. 533-581.

Noble, M. and B. Butman (1979). Low-frequency Wind-induced Sea Level Oscillations along the East Coast of North America. J. of Geophysical Research, 84 (C6), pp. 3227-3236.

Papoulis, 1962.

Peterssen, S. (1969). Introduction to Meteorology. McGraw-Hill, New York.

Smith, S.D., and E.G. Banke (1975). Variation of the Sea Surface Drag Coefficient with Wind Speed. Quart. J. Roy. Met. Soc., 101, pp. 665-673.

Steeves, R.R. (1981a). Least Squares Response Analysis and its Application to Tiltmeter Observations. Ph.D. Thesis, University of New Brunswick.

Steeves, R.R. (1981b). Users Manual for Program SPANER: Least Squares Spectral and Response Analysis of Equally Spaced Time Series. University of New Brunswick, Dept. of Surveying Engineering, Technical Report, in preparation.

Steeves, R.R. (1981c). A Statistical Test for Significance of Peaks in the Least Squares Spectrum. Submitted to Manuscripta Geodaetica.

Taylor, J. and S. Hamilton (1972). Some Tests of the Vanicek Method of Spectral Analysis. Astrophysics and Space Science, 17, pp. 357-367.

Thompson, K.R. (1979). Regression Models for Monthly Mean Sea Level. Marine Geodesy, 2(3), pp. 269-290.

Vanicek, P. (1971). Further Development and Properties of the Spectral Analysis by Least Squares. Astrophysics and Space Science, 12 (1971), pp. 10-33.

Vanicek, P. (1978). To the Problem of Noise Reduction in Sea-Level Records Used in Vertical Crustal Movement Detection. Physics of the Earth and Planetary Interiors, 17, pp. 265-280.

Wang, D.P. (1975). Low Frequency Sea Level Variability on the Middle Atlantic Bight. J. of Marine Research, 37 (4), pp. 683-697.

Wells, D.E. and P. Vanicek (1978). Least Squares Spectral Analysis. Bedford Institute of Oceanography, Report BI-R-78-8.

Willebrand, J. (1978). Temporal and Spatial Scales of the Wind Field over the North Pacific and North Atlantic. J. of Physical Oceanography, 8, pp. 1080-1094.

Wunsch, C. (1972). Bermuda Sea Level in Relation to Tides, Weather and Baroclinic Fluctuations - Reviews of Geophysics and Space Science, 10 (1), pp. 1-49.